with standard-dose AraC consolidation and 62% with high-dose AraC consolidation. As the AML201 study included patients with core-binding factor AML (28% of the total population), and the patients in that study were selected according to the pre-defined inclusion and exclusion criteria, it is remarkable that a comparable survival rate was achieved in our patients. The active use of allogeneic HCT not only in patients with a related donor but also in those without a related donor likely contributed to the favorable overall outcome of our patients.

In contrast to the results of meta-analysis studies of the prospective donor vs no-donor comparison,[8–10] our patients with and without a related donor had comparable OS. Similar results were obtained if the outcome was compared in terms of RFS (data not shown). The most likely explanations for this result is that up to 41% of our patients without a related donor proceeded to unrelated HCT during CR1, and that OS after allogeneic HCT in CR1 did not differ between patients with and without a related donor. NRM is a major obstacle to the success of unrelated HCT. Early studies showed less satisfactory results with unrelated HCT because of a high incidence of NRM.[13,14] However, according to more recent data, comparable outcomes have been reported for related and unrelated HCT in AML patients.[15–18] In our study, the cumulative incidence of NRM in patients undergoing unrelated HCT was significantly higher than that in those undergoing related HCT (21% vs 13%, $P=0.022$), but the NRM rate of 21% with unrelated HCT appears to be within the acceptable range. The benefits of unrelated HCT may be increased by reducing NRM with the aid of stricter matching between donor and patient, increasing the use of reduced-intensity conditioning, and applying better supportive care. Recently, several groups have conducted prospective donor vs no-donor studies for AML patients with high-risk features by expanding the type of donor to include unrelated donors.[19–21] Notably, despite a limited number of patients in each study, they showed significantly superior OS in patients with a donor, as well as comparable OS in patients undergoing related and unrelated HCT.[19–21] These prospective studies also support the usefulness of unrelated HCT in younger AML patients with non-favorable cytogenetics. Although our multivariate analysis showed that the degree to which allogeneic HCT had favorably affected outcome was less marked in patients without a related donor compared with those with a related donor, unrelated HCT could be considered a reasonable treatment option if a related donor is not available.

When our data are interpreted, it should be remembered that this study was an observational study, not an interventional study. The decision of whether or not to proceed to allogeneic HCT could be confounded by multiple factors, and early relapse, for example, did not seem to be a main cause for not having undergone allogeneic HCT during CR1 in our study. Adjusting for known confounding factors by using a multivariate analysis cannot guarantee that biases are removed. Thus, the results presented here need to be interpreted cautiously. Although we acknowledge such a limitation, our data showed that related donor availability did not significantly affect OS in younger patients with cytogenetically non-favorable AML. We consider this was because 41% of the patients without a related donor underwent unrelated HCT during CR1, and the outcome after transplantation was comparable between related and unrelated HCT. These results show the usefulness of unrelated HCT in this patient population when they do not have a related donor. The extensive use of unrelated HCT for such patients may minimize the potential disadvantage of lacking a related donor.

CONFLICT OF INTEREST

The authors declare no conflict of interest.

ACKNOWLEDGEMENTS

This work was supported by grants from the Japanese Ministry of Health, Labour and Welfare and the National Cancer Research and Development Fund (23-A-28).

Author contributions: MY designed the study, interpreted data, and wrote the manuscript; SK prepared the data file, performed the analysis and interpreted data; TY was primarily responsible for the study design, data analysis and interpretation of the data; NU, SM, HK, KU, TK, MW, KN, SY, Y Nawa, JT, HT, Y Nakamura, SF and FK obtained the patients' data and interpreted data; NE designed the study and interpreted data; IM reviewed the cytogenetic reports and interpreted data; and TF interpreted data and helped to write the manuscript.

REFERENCES

1 Gupta V, Tallman MS, Weisdorf DJ. Allogeneic hematopoietic cell transplantation for adults with acute myeloid leukemia: myths, controversies, and unknowns. *Blood* 2011; **117**: 2307–2318.
2 Reiffers J, Stoppa AM, Attal M, Michallet M, Marit G, Blaise D *et al.* Allogeneic vs autologous stem cell transplantation vs chemotherapy in patients with acute myeloid leukemia in first remission: the BGMT 87 study. *Leukemia* 1996; **10**: 1874–1882.
3 Keating S, de Witte T, Suciu S, Willemze R, Hayat M, Labar B *et al.* The influence of HLA-matched sibling donor availability on treatment outcome for patients with AML: an analysis of the AML 8A study of the EORTC Leukaemia Cooperative Group and GIMEMA. European Organization for Research and Treatment of Cancer. Gruppo Italiano Malattie Ematologiche Maligne dell'Adulto. *Br J Haematol* 1998; **102**: 1344–1353.
4 Slovak ML, Kopecky KJ, Cassileth PA, Harrington DH, Theil KS, Mohamed A *et al.* Karyotypic analysis predicts outcome of preremission and postremission therapy in adult acute myeloid leukemia: a Southwest Oncology Group/Eastern Cooperative Oncology Group Study. *Blood* 2000; **96**: 4075–4083.
5 Burnett AK, Wheatley K, Goldstone AH, Stevens RF, Hann IM, Rees JH *et al.* The value of allogeneic bone marrow transplant in patients with acute myeloid leukaemia at differing risk of relapse: results of the UK MRC AML 10 trial. *Br J Haematol* 2002; **118**: 385–400.
6 Suciu S, Mandelli F, de Witte T, Zittoun R, Gallo E, Labar B *et al.* Allogeneic compared with autologous stem cell transplantation in the treatment of patients younger than 46 years with acute myeloid leukemia (AML) in first complete remission (CR1): an intention-to-treat analysis of the EORTC/GIMEMAAML-10 trial. *Blood* 2003; **102**: 1232–1240.
7 Sakamaki H, Miyawaki S, Ohtake S, Emi N, Yagasaki F, Mitani K *et al.* Allogeneic stem cell transplantation versus chemotherapy as post-remission therapy for intermediate or poor risk adult acute myeloid leukemia: results of the JALSG AML97 study. *Int J Hematol* 2010; **91**: 284–292.
8 Cornelissen JJ, van Putten WL, Verdonck LF, Theobald M, Jacky E, Daenen SM *et al.* Results of a HOVON/SAKK donor versus no-donor analysis of myeloablative HLA-identical sibling stem cell transplantation in first remission acute myeloid leukemia in young and middle-aged adults: benefits for whom? *Blood* 2007; **109**: 3658–3666.
9 Yanada M, Matsuo K, Emi N, Naoe T. Efficacy of allogeneic hematopoietic stem cell transplantation depends on cytogenetic risk for acute myeloid leukemia in first disease remission: a metaanalysis. *Cancer* 2005; **103**: 1652–1658.
10 Koreth J, Schlenk R, Kopecky KJ, Honda S, Sierra J, Djulbegovic BJ *et al.* Allogeneic stem cell transplantation for acute myeloid leukemia in first complete remission: systematic review and meta-analysis of prospective clinical trials. *JAMA* 2009; **301**: 2349–2361.
11 Vardiman JW, Thiele J, Arber DA, Brunning RD, Borowitz MJ, Porwit A *et al.* The 2008 revision of the World Health Organization (WHO) classification of myeloid neoplasms and acute leukemia: rationale and important changes. *Blood* 2009; **114**: 937–951.
12 Miyawaki S, Ohtake S, Fujisawa S, Kiyoi H, Shinagawa K, Usui N *et al.* A randomized comparison of 4 courses of standard-dose multiagent chemotherapy versus 3 courses of high-dose cytarabine alone in postremission therapy for acute myeloid leukemia in adults: the JALSG AML201 Study. *Blood* 2011; **117**: 2366–2372.
13 Szydlo R, Goldman JM, Klein JP, Gale RP, Ash RC, Bach FH *et al.* Results of allogeneic bone marrow transplants for leukemia using donors other than HLA-identical siblings. *J Clin Oncol* 1997; **15**: 1767–1777.
14 Lazarus HM, Perez WS, Klein JP, Kollman C, Bate-Boyle B, Bredeson CN *et al.* Autotransplantation versus HLA-matched unrelated donor transplantation for acute myeloid leukaemia: a retrospective analysis from the Center for International Blood and Marrow Transplant Research. *Br J Haematol* 2006; **132**: 755–769.
15 Moore J, Nivison-Smith I, Goh K, Ma D, Bradstock K, Szer J *et al.* Equivalent survival for sibling and unrelated donor allogeneic stem cell transplantation for acute myelogenous leukemia. *Biol Blood Marrow Transplant* 2007; **13**: 601–607.

16 Schetelig J, Bornhauser M, Schmid C, Hertenstein B, Schwerdtfeger R, Martin H *et al.* Matched unrelated or matched sibling donors result in comparable survival after allogeneic stem-cell transplantation in elderly patients with acute myeloid leukemia: a report from the cooperative German Transplant Study Group. *J Clin Oncol* 2008; **26**: 5183–5191.
17 Gupta V, Tallman MS, He W, Logan BR, Copelan E, Gale RP *et al.* Comparable survival after HLA-well-matched unrelated or matched sibling donor transplantation for acute myeloid leukemia in first remission with unfavorable cytogenetics at diagnosis. *Blood* 2010; **116**: 1839–1848.
18 Walter RB, Pagel JM, Gooley TA, Petersdorf EW, Sorror ML, Woolfrey AE *et al.* Comparison of matched unrelated and matched related donor myeloablative hematopoietic cell transplantation for adults with acute myeloid leukemia in first remission. *Leukemia* 2010; **24**: 1276–1282.
19 Basara N, Schulze A, Wedding U, Mohren M, Gerhardt A, Junghanss C *et al.* Early related or unrelated haematopoietic cell transplantation results in higher overall survival and leukaemia-free survival compared with conventional chemotherapy in high-risk acute myeloid leukaemia patients in first complete remission. *Leukemia* 2009; **23**: 635–640.
20 Schlenk RF, Dohner K, Mack S, Stoppel M, Kiraly F, Gotze K *et al.* Prospective evaluation of allogeneic hematopoietic stem-cell transplantation from matched related and matched unrelated donors in younger adults with high-risk acute myeloid leukemia: German-Austrian trial AMLHD98A. *J Clin Oncol* 2010; **28**: 4642–4648.
21 Stelljes M, Beelen DW, Braess J, Sauerland MC, Heinecke A, Berning B *et al.* Allogeneic transplantation as post-remission therapy for cytogenetically high-risk acute myeloid leukemia: landmark analysis from a single prospective multicenter trial. *Haematologica* 2011; **96**: 972–979.

STEM CELLS®
TISSUE-SPECIFIC STEM CELLS

Individual Hematopoietic Stem Cells in Human Bone Marrow of Patients with Aplastic Anemia or Myelodysplastic Syndrome Stably Give Rise to Limited Cell Lineages

TAKAMASA KATAGIRI,[a,b] HIROSHI KAWAMOTO,[c] TAKASHI NAKAKUKI,[d] KEN ISHIYAMA,[b] MARIKO OKADA-HATAKEYAMA,[e] SHIGEKI OHTAKE,[a] YU SEIKI,[b] KOHEI HOSOKAWA,[b] SHINJI NAKAO[b]

[a]Clinical Laboratory Science, Division of Health Sciences, and Kanazawa University Graduate School of Medical Science, Kanazawa, Ishikawa, Japan; [b]Cellular Transplantation Biology, Kanazawa University Graduate School of Medical Science, Kanazawa, Ishikawa, Japan; [c]Laboratory for Lymphocyte Development and [e]Laboratory for Cellular Systems Modeling, RIKEN Research Center for Allergy and Immunology, Tsurumi-ku, Yokohama, Kanagawa, Japan RIKEN Research Center for Allergy and Immunology, Tsurumi-ku, Yokohama, Kanagawa, Japan; [d]Department of Mechanical Systems Engineering Faculty of Engineering, Kogakuin University, Shinjuku-ku, Tokyo, Japan.

Key Words. Differentiation • Experimental models • Fluorescence-activated cell sorting • Hemopoietic stem cells • Hematopoietic progenitors • Aplastic anemia • Bone marrow

ABSTRACT

Mutation of the phosphatidylinositol *N*-acetylglucosaminyltransferase subunit A (*PIG-A*) gene in hematopoietic stem cells (HSCs) results in the loss of glycosylphosphatidylinositol-anchored proteins (GPI-APs) on HSCs, but minimally affects their development, and thus can be used as a clonal maker of HSCs. We analyzed GPI-APs expression on six major lineage cells in a total of 574 patients with bone marrow (BM) failure in which microenvironment itself is thought to be unaffected, including aplastic anemia (AA) or myelodysplastic syndrome (MDS). GPI-APs-deficient (GPI-APs$^-$) cells were detected in 250 patients. Whereas the GPI-APs$^-$ cells were seen in all six lineages in a majority of patients who had higher proportion ([dbmtequ]3%) of GPI-APs$^-$ cells, they were detected in only limited lineages in 92.9% of cases in the lower proportion (<3%) group. In all 250 cases, the same lineages of GPI-APs$^-$ cells were detected even after 6–18-month intervals, indicating that the GPI-APs$^-$ cells reflect hematopoiesis maintained by a self-renewing HSC in most of cases. The frequency of clones with limited lineages seen in mild cases of AA was similar to that in severe cases, and clones with limited lineages were seen even in two health volunteer cases. These results strongly suggest most individual HSCs produce only restricted lineages even in a steady state. While this restriction could reflect heterogeneity in the developmental potential of HSCs, we propose an alternative model in which the BM microenvironment is mosaic in supporting commitment of progenitors toward distinct lineages. Our computer simulation based on this model successfully recapitulated the observed clinical data. STEM CELLS *2013;31:536–546*

Disclosure of potential conflicts of interest is found at the end of this article.

INTRODUCTION

To sustain hematopoiesis, hematopoietic stem cells (HSCs) must, on the one hand, replenish themselves by self-renewal and on the other hand produce differentiating progenitor cells. It is also known that most HSCs remain dormant and are only rarely and randomly activated. It has been estimated that each human possesses a total of 10^4 HSCs, and that ~400 HSCs actively contribute to hematopoiesis, replicating once per year [1, 2]. However, the actual dynamics of hematopoiesis by HSCs remains uncertain. For example, it is unclear how long an individual HSC maintains hematopoiesis and whether all major lineage cells are produced from a single HSC. These issues have been difficult to address due to the lack of appropriate experimental systems, regardless of animal species.

In the case of humans, however, we were led to consider one "experiment of nature" that makes it possible to track the

Author contributions: H.K.: developed the concept of the study and supervised the project, designed the experiments, wrote the paper, and approved the final version of this paper; S.N.: developed the concept of the study and supervised the project, wrote the paper, and approved the final version of this paper; T.K. and T.N.: designed the experiments, performed the experiments and analyzed the data, wrote the paper, and approved the final version of this paper; K.I. and M.O.-H.: designed the experiments and approved the final version of this paper; S.O., Y.S. and K.H. :performed the experiments and analyzed the data, approved the final version of this paper. T.K., H.K., and T.N. contributed equally to this article.

Correspondence: Shinji Nakao, M.D., Ph.D., Cellular Transplantation Biology, Kanazawa University Graduate School of Medical Science, 13-1 Takara-machi, Kanazawa, Ishikawa 920-8640, Japan. Telephone: +81-76-265-2274; Fax: +81-76-234-4252; e-mail: snakao8205@staff.kanazawa-u.ac.jp Received September 21, 2012; Revised November 12, 2012; accepted for publication November 26, 2012; first published online in STEM CELLS *EXPRESS* January 12, 2013. 1066-5099/2013/$30.00/0 doi: 10.1002/stem.1301

progeny of a HSC; that is, by detecting blood cells deficient in glycosylphosphatidylinositol-anchored proteins (GPI-APs) using flow cytometry. GPI-APs-deficient (GPI-APs$^-$) blood cells are rarely detectable in healthy individuals, but are a common feature in paroxysmal nocturnal hemoglobinuria (PNH) and are also frequently seen in patients with bone marrow (BM) failure such as aplastic anemia (AA) or myelodysplastic syndrome (MDS). These cells are known to be derived from HSCs with a mutation in the phosphatidylinositol *N*-acetylglucosaminyltransferase subunit A (*PIG-A*) gene. MDS cases harboring GPI-APs$^-$ blood cells are characterized by polyclonal hematopoiesis and good response to immunosuppressive therapy, and are therefore thought to be similar to AA in their pathophysiology [3].

The *PIG-A* mutant HSCs used to be thought to have greater proliferative capacity than normal HSCs because one or a few *PIG-A* mutant clones sometimes account for a large proportion of hematopoietic cells for long period in PNH patients [4]. However, several reports instead indicate that the mutant HSCs in most PNH patients have properties similar to normal HSCs: for example, no growth advantage over wild-type HSCs [5, 6], genetic stability and extremely low incidence of secondary mutations [2, 7–9], and the rarity of leukemic cell evolution of GPI-APs$^-$ cells in PNH patients [10].

We recently found that GPI-APs$^-$ cells in patients with AA and MDS frequently show various patterns in the proportion of granulocytes and erythrocytes and that the individual patterns of the two lineage combinations can persist for many years. The percentage of GPI-APs$^-$ cells in some patients remained almost the same over 10 years even when the percentages were less than 1% [11]. In such stable cases, it is quite likely that GPI-APs$^-$ peripheral blood (PB) cells are produced from HSC(s), and that the GPI-APs$^-$ HSC itself as well as its surrounding environment is largely normal, at least during the observation period. Indeed, BM environment itself in the patients to support hematopoiesis is thought to be largely normal, since these cases are thought to be caused by immune reaction against blood cells. It is also highly probable that the whole GPI-APs$^-$ cells in each patient represent a clone, originating from a single HSC in which *PIG-A* mutation occurred, since it is statistically rare that the *PIG-A* mutation occurs twice in one patient. Although it is unclear that such a clone is maintained by a single HSC or multiple descendent HSCs, it can be said that the kinetics of GPI-APs$^-$ cells during stable period reflect the regular hematopoietic events originally initiated by a single HSC. We then thought that it could be very much informative if we extend our analysis to cover various hematopoietic lineages in addition to erythrocytes and granulocytes. We therefore determined the proportion of GPI-APs$^-$ cells in six major lineages, namely granulocytes (G), monocytes (M), erythrocytes (E), T cells (T), Natural Killer cells (NK), and B cells (B), in PB cells from BM failure patients using a highly sensitivity flow cytometric analysis [12].

Materials and Methods

Patients and Healthy Volunteers

The PB of 574 patients with various types of cytopenias was examined for the presence of GPI-APs$^-$ cells using high sensitivity flow cytometry. Their diagnoses included AA in 354 (39 with very severe, 92 with severe, and 223 with nonsevere AA [13]), MDS-refractory anemia (RA) defined by the french-american-british (FAB) classification [14] in 207, and classic PNH in 13. The male to female ratio was 1:1.2 (261:313) and the median age was 57 years (range: 1–95 years). PB samples from 192 healthy individuals were also examined for the presence of GPI-APs$^-$ cells in all lineages of cells. All patients and healthy individuals including next of kin on the behalf of minors/children participants in our study provided their informed written consent before sampling. This study protocol was approved by the ethics committee of Kanazawa University Graduate School of Medical Science.

Monoclonal Antibodies

Monoclonal antibodies (mAbs) used for multicolor flow cytometry were anti-CD59 labeled with FITC (P282E, IgG2a; Beckman Coulter, Miami, FL, http://www.labome.com/product/Beckman-Coulter-Inc/IM3457U.html), anti-CD55 labeled with FITC (IA10, IgG2a; BD Pharmingen,http://www.bdbiosciences.com/external_files/pm/doc/tds/human/live/web_enabled/33574X_555693.pdf), anti-CD48 labeled with FITC (J4-57, IgG1; Beckman Coulter, http://www.bionity.com/en/antibodies/beckman-IM1837U/cd48-anti-human-klon-j4-57.html), anti-CD33 labeled with APC (D3HL60.251, IgG1; Beckman Coulter, http://www.bionity.com/en/antibodies/beckman-A70200/cd33-anti-human-klon-d3hl60-251.html), anti-CD19 labeled with APC-Cy7 (SJ25C1, IgG1; BD Pharmingen, http://www.bdbiosciences.com/external_files/pm/doc/tds/human/live/web_enabled/557791.pdf), anti-CD335 labeled with Phycoerythrin (BAB281, IgG1; Beckman Coulter, http://www.bc-cytometry.com/DataSheetPDF/IM3711_D.S.pdf), anti-CD3 labeled with PerCPCy5.5 (SK7, IgG1; BD Pharmingen, http://www.bdbiosciences.com/documents/BD_PerCP-Cy5.5_and_PerCP.pdf), anti-CD11b/Mac-1 labeled with PE (ICRF44, IgG1; BD Pharmingen, http://www4.bdj.co.jp/ecat/txDetailedTable.jsp?size=20&item=746256&form=formNavigator&action=LIST_PAGE&pageItem=45), and anti-glycophorin A labeled with PE (JC159, IgG1; Dako, Carpenteria, CA, http://www.dako.com/us/index/flow_cytometry_catalog_us.pdf).

Flow Cytometry for Detecting GPI-APs$^-$ Cells

Six lineages of blood cells including granulocytes, erythrocytes, monocytes, T cells, B cells, and NK cells were subjected to high sensitivity flow cytometry for detecting small populations of GPI-APs$^-$ cells. All blood samples were analyzed within 24 hours to avoid false-positive results due to cell damage. The staining with the each mAb in this study was performed according to the well-established lyse-stain protocol, previously described in detail [12, 15]. Briefly, 3–5 mL of heparinized blood was drawn from the patients and healthy individuals. Erythrocytes were lysed in a lysis buffer (Roche Applied Science, Nagoya, Japan, http://roche-biochem.jp/catalog/index.php/product_3.6.6.4.42.1.html) containing NH_4Cl 8.26 g/L, $KHCO_3$ 1.0 g/L, and EDTA·E_4Na 0.037 g/L to detect GPI-APs$^-$ leukocytes. After washing with saline, 50 μL of the leukocyte suspension was incubated with FITC-labeled anti-CD55 and anti-CD59 mAbs for granulocytes or FITC-labeled anti-CD48 and anti-CD59 mAbs for monocytes, T cells, B cells, and NK cells in combination with mAbs specific for lineage markers including PE-labeled CD11b for granulocytes, APC-labeled CD33 for monocytes, PerCP-Cy5.5-labeled CD3 for T cells, APC-Cy7-labeled CD19 for B cells, and PE-labeled CD335 for NK cells. Fresh blood was diluted to 3% in phosphate-buffered saline (PBS), and then 50 μL was incubated with PE-labeled anti-glycophorin A and FITC-labeled anti-CD55 and anti-CD59 mAbs on ice for 30 minutes to detect GPI-APs$^-$ erythrocytes. Three-step gating excluded debris and immature granulocytes that are frequently found in samples from patients with MDS. Step 1 involved the gating of granulocyte, lymphocyte, or monocyte populations from the Forward Scatter (FSC)-Side Scatter (SSC) scattergrams (R1). Step 2 involved the gating of the lineage marker^{bright} population on the lineage marker-SSC scattergram to exclude the lineage marker^{dim} cells that are features of either damaged cells or immature cells. Step 3 was the gating of R1 × R2 and the analysis of 10^6 cells on R1 × R2 scattergrams. The following cut-off values that had been determined by our

previous studies based on 183 healthy individuals were used; the presence of ≥0.005% $CD55^-CD59^-$ glycophorin A^+ erythrocytes, ≥0.003% $CD55^-CD59^-CD11b^+$ granulocytes, and ≥0.01% $CD48^-CD59^-CD33^+$ monocytes, $CD48^-CD59^-CD3^+$ T cells, $CD48^-CD59^-CD19^+$ B cells, and $CD48^-CD59^-CD335^+$ NK cells [12, 16]. When GPI-APs$^-$ cells were detected in only one lineage of cells or the percentages of GPI-APs$^-$ cells were less than 0.01%, then additional samples were tested, and the patients were judged to be positive for increased GPI-APs$^-$ (PNH^+) when the analysis results of the first and second samples were identical. Data acquisition was performed immediately after the sample preparation using a FACSCanto II instrument (Beckton Dickinson) and the data were analyzed using the FACSDiva software program and the percentage of each population was calculated by FlowJo software 7.6.1 (Tree star, Inc., Ashland, OR).

Cell Sorting and *PIG-A* Gene Analysis

Freshly isolated GPI-APs$^-$ cells were separated from GPI-APs$^+$ fraction using a FACSAria II instrument (Beckton Dickinson). More than 95% of the sorted cells were GPI-APs deficient. An analysis of the *PIG-A* gene mutation was performed as described previously [17]. Briefly, the coding regions of *PIG-A* were amplified by nested or seminested PCR using 12 primer sets, and six ligation reactions were used to transform competent *Escherichia coli* JM109 cells (Nippon Gene, Japan, http://www.nippongene.com/pages/products/genetransfer/ecos/index.html). Five clones were selected randomly from each group of transfectants and subjected to sequencing with BigDye Terminator v3.1 Cycle Sequencing kit (Applied Biosystems, San Diego, CA,http://www3.appliedbiosystems.com/cms/groups/mcb_support/documents/generaldocuments/cms_042772.pdf) and an ABI PRISM 3100 Genetic Analyzer (Applied Biosystems).

Simulation of the Blood Cell Production by HSCs

Migration, division, lineage determination, and death of clones of a HSC in BM environment are simulated with a lattice Monte Carlo method. For efficient simulation, we focused on the events on a cross-section of BM, which enabled us to perform two-dimensional simulation. The occurrence of events was managed with their transition probabilities and the simulation was executed on the basis of actual time. We used the hybrid null-event Monte Carlo algorithm [18, 19], and here outline the model description and simulation setup (also see Supporting Information Note for detailed information). A square area (30 mm × 30 mm) that is large enough to encompass some commitment planes is represented using 1,500 × 1,500 square lattices (20 μm × 20 μm each). Initially, a HSC is randomly added to a site, and then it continues to create clones once per 10 hours until there have been five divisions. Clones randomly move along the lattice with the transition probability and undergo cell division once per 8–12 hours. We assume that lineage determination occurs after the fifth division, based on the site of the clone in the mosaic-like hematopoietic environment where each site supports differentiation into M, E, B, or T-cell lineages. In addition, the lineage clone becomes a mature cell after a further five divisions under the condition that it can divide only in the sites that support differentiation into the same lineage. Otherwise, cell death results after 48-hour movement on areas that support other lineages, although all clones die 72 hours after maturation.

We also investigated the relation between clone size and the number of emerging cell lineages. In our simulation, clone size is dominated by the setting of "N times divisions for lineage determination and further N times divisions for maturing." We simply change the number N in a range of 3–12. For each N, 128 simulations starting from randomly selected initial sites of HSCs are executed for 120 simulation hours. For each simulation, the number of cell lineages is counted, and clone size is calculated as the maximum number of clones for the entire simulation period.

Results

GPI-APs$^-$ Cells Were Seen in Various Combination of Lineages of Blood Cells from BM Failure Patients

Of 574 patients with BM failure, GPI-APs$^-$ cells were detected in at least one lineage of cells of 250 patients (44%). The prevalences of increased GPI-APs$^-$ cells were 56% in AA and 19% in MDS-RA. The proportion of GPI-APs$^-$ cells among granulocytes ranged 0.003%–99.1%, with mean and median value 5.38% and 0.19%, respectively. GPI-APs$^-$ cells were rather frequently found in patients with less severe AA; the prevalences were 63% in nonsevere, 49% in severe, and 31% in very severe AA patients. The lineage combinations of GPI-APs$^-$ cells in patients possessing GPI-APs$^-$ cells (PNH^+ patients) were classified into 16 different patterns (Supporting Information Table S1). Figure 1 shows representative flow cytometric profiles of one healthy individual and four patients showing Granulocyte, Monocyte, Erythrocyte, T cell, NK cell, B cell (GMETNKB), Granulocyte, Monocyte, Erythrocyte (GME), Granulocyte, Monocyte, Erythrocyte, T cell, NK (GMETNK), or Granulocyte, Monocyte, Erythrocyte, B cell (GMEB) patterns.

Clone Size of GPI-APs$^-$ Granulocytes Correlates with the Number of Cell Lineages that Contain GPI-APs$^-$ Cells

The percentages of GPI-APs$^-$ granulocytes in each group bearing GPI-APs$^-$ cells in one to six lineages are plotted in Figure 2. There was a clear trend toward the pattern of the higher the percentage of GPI-APs$^-$ granulocytes in patients, the greater the number of GPI-APs$^-$ cell lineages.

In order to closely examine the relationship between the severity of AA and the GPI-APs$^-$ clone size, we arbitrarily classified AA patients in this study into five categories, namely stages 1, 2, and 3 (nonsevere), stage 4 (severe), and stage 5 (very severe), based on the severity of cytopenias (Supporting Information Table S2) and replotted the data (Fig. 2B). Patients with higher proportion (>1%) of GPI-APs$^-$ granulocytes were not seen in nonsevere cases, suggesting that the clone size of GPI-APs$^-$ cells correlates with severity of BM failure. The notable observation here is that the correlation between the percentage of GPI-APs$^-$ granulocytes and the number of GPI-APs$^-$ cell lineages is almost identical in all three groups. This finding may indicate that the production of limited lineage cells observed in smaller clones is not due to the possible functional failures of BM microenvironment. It seems more likely that "fewer lineages in smaller clones" instead represents events occurring in normal hematopoiesis.

Persistence of GPI-APs$^-$ Lineage Combination Over a Long Period

We then reexamined PB cells of 250 patients 6–18 months after the first examination and to our surprise, GPI-APs$^-$ cells were observed in all 250 patients. Detection of GPI-APs$^-$ cells after such a long interval indicates that the GPI-APs$^-$ cells are most likely derived from HSCs rather than from non-self-renewing progenitors. Of special interest was our finding that in all 250 cases, the same combinations of lineages were detected regardless of the interval between the first and second analysis. Flow cytometric profiles of various lineages of a case representing Granulocyte, Monocyte, Erythrocyte, T cell (GMET) type are shown in Figure 3. Figure 4 shows the proportion of GPI-APs$^-$ cells in each lineage in the first and second analysis for a total of representative 25 cases (five cases for each type).

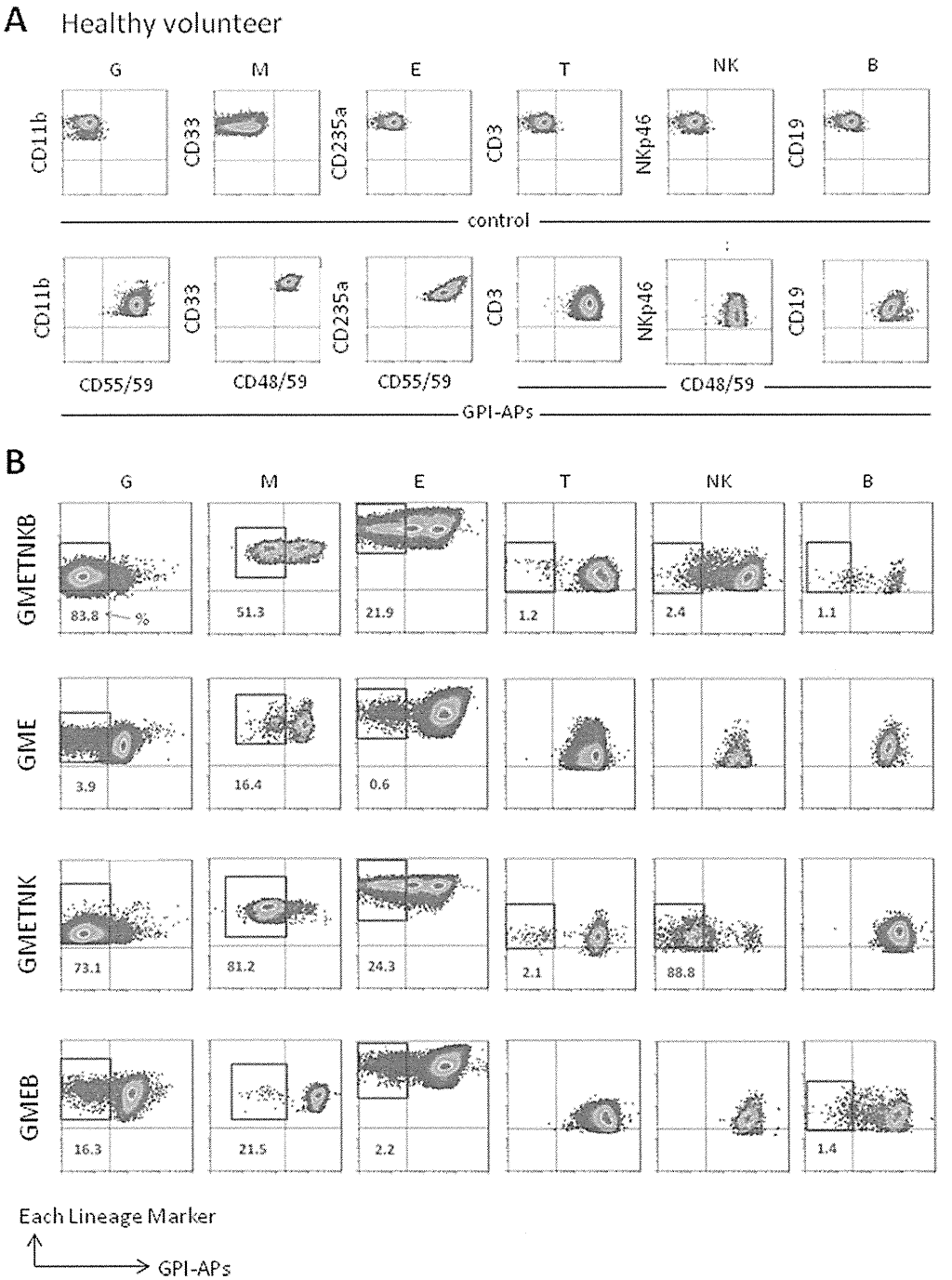

Figure 1. Detection of GPI-APs$^-$ cells in different lineages of blood cells. **(A):** One example of peripheral blood (PB) cells of a healthy individual having no GPI-APs$^-$ cells. **(B):** GPI-APs$^-$ cell combination patterns in four patients. Profiles of PB cells of patients showing GPI-APs$^-$ cells in GMETNKB, GME, GMETNK, and GMEB lineages are shown. Lineage markers used were CD11b for G, CD33 for M, glycophorin-A (CD235a) for E, CD3 for T, NKp46 for NK, and CD19 for B. G, M, E, T, NK, or B stands for granulocytes, monocytes, erythrocytes, T cells, NK cells, or B cells, respectively. Abbreviations: GPI-APs, glycosylphosphatidylinositol-anchored proteins; GME, Granulocyte, Monocyte, Erythrocyte.

PIG-A Gene Mutations in Different Lineages of Blood Cells

To confirm their clonal origin, GPI-APs$^-$ cells sorted from five patients were subjected to *PIG-A* gene analysis. The same mutation was identified in different lineages in three patients (Supporting Information Table S3). In GPI-APs$^-$ granulocytes with other lineages from Patients 16, 1, and 5 and GPI-APs$^-$ granulocytes from Patients 9 and 30, the same

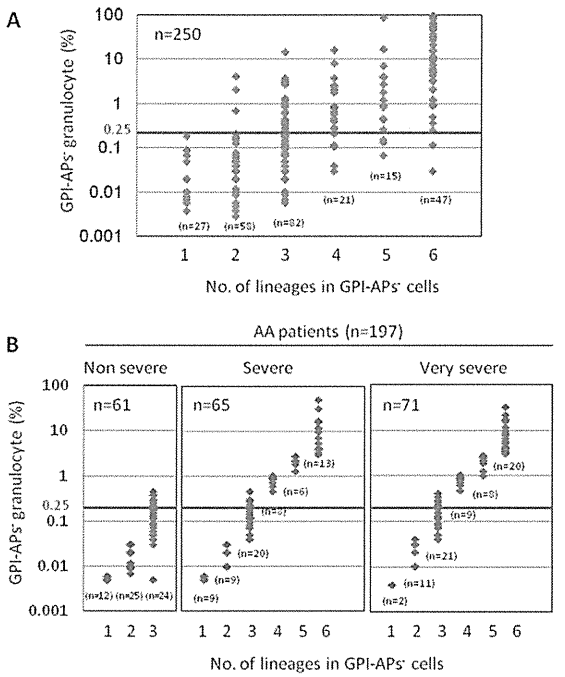

Figure 2. Correlation between the clone size of GPI-APs$^-$ granulocytes and the number of cell lineages that contain GPI-APs$^-$ cells. **(A):** The percentage of GPI-APs$^-$ granulocytes and the number of cell lineages that contain GPI-APs$^-$ cells in individual patients are plotted. A red line for 0.25% stands for the expected value for an average size of a single hematopoietic stem cell clone. **(B):** The percentage of GPI-APs$^-$ granulocytes and the number of cell lineages that contain GPI-APs$^-$ cells in AA patients, classified in three categories according to the severity of disease (stage 1 or 2, stage 3, and stage 4 or 5), are plotted. AA patients were classified into five categories based on the disease severity (stage 1 or 2, stage 3, and stage 4 or 5) (Supporting Information Table S2). Abbreviation: GPI-APs, glycosylphosphatidylinositol-anchored proteins.

mutation was found 3–7 months after the initial analyses. Therefore, it is highly probable that in most, if not all, cases the GPI-APs$^-$ cells are clonal [20]. This finding is in line with the estimation that PNH patients only rarely have more than two clones at the HSC level [8, 9].

GPI-APs$^-$ Cells Were Detected in Limited Lineages in Healthy Volunteers Over a Long Period

Dormant HSCs with *PIG-A* mutation reside in the BM and can be activated albeit uncommonly [17]. If this hypothesis is tenable, small populations of GPI-APs$^-$ cells may be detectable in some healthy individuals. We then examined PB of 192 healthy volunteers for the presence of GPI-APs$^-$ cells. Notably, two were found to bear detectable levels of GPI-APs$^-$ cells, and in both of them GPI-APs$^-$ cells were detected in limited lineages, representing GME and GE type (Fig. 5A). The two healthy cases bearing GPI-APs$^-$ cells were situated within the range of distribution of AA and MDS cases in terms of chimerism ratio versus lineage number (Fig. 5B), further supporting that findings seen in AA and MDS cases reflect normal hematopoiesis.

As described in Introduction, the number of active human HSCs at any given time is estimated to be around 400. It is therefore likely that the GPI-APs$^-$ clones with a frequency of less than 0.25% reflect hematopoiesis maintained by a single HSC. It is clear from our studies that most of these small clones contain only limited lineage cells. Even in the case of larger clones, for example, clones of 1%–3% chimerism that might be maintained more than two HSCs, the majority (81%) are non-full-lineage clones. Collectively, these results indicate that most individual human HSCs only give rise to a limited range of hematopoietic progeny.

A Model for the Hematopoietic Microenvironment to Explain the Production of Limited Cell Lineages from a HSC

A cogent explanation for this phenomenon may have important implications for normal hematopoiesis. We

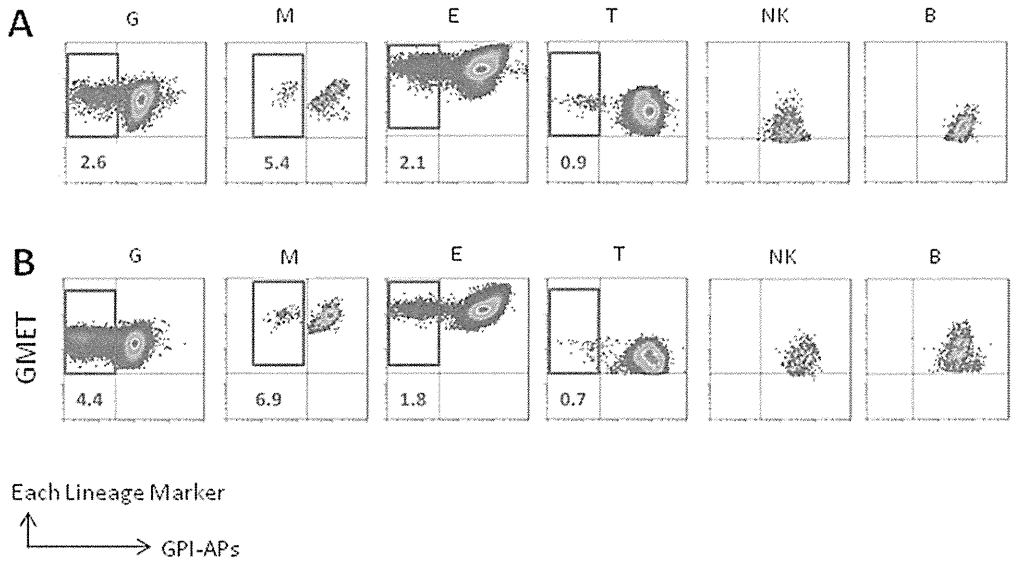

Figure 3. The lineage combination pattern of GPI-APs$^-$ cells was same at the first sampling **(A)** and after 6 months **(B)**. Abbreviation: GPI-APs, glycosylphosphatidylinositol-anchored proteins.

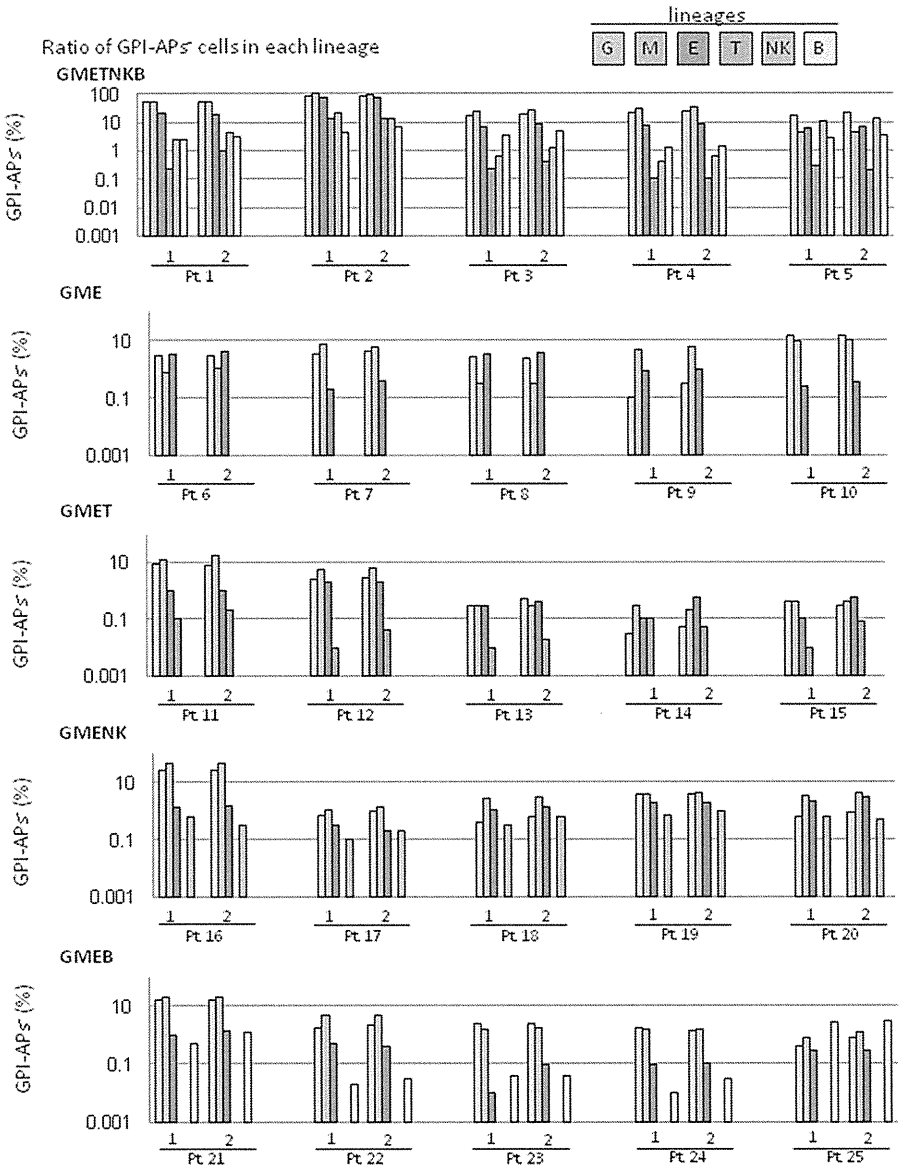

Figure 4. The combination of GPI-APs⁻ lineage as well as the proportion of GPI-APs⁻ cells in peripheral blood (PB) persists over a long period. GPI-APs⁻ cells were analyzed in PB of 250 patients twice at intervals ranging 6–18 months. The numbers 1 and 2 refer to the first and second analysis. In all cases, GPI-APs⁻ cells were detected in the same lineages in both analyses. Among them, 25 cases (five for each type of lineage combination) are shown. Bars represent the proportion of GPI-APs⁻ cells in each lineage in PB. Abbreviations: GPI-APs, glycosylphosphatidylinositol-anchored proteins; GMET, Granulocyte, Monocyte, Erythrocyte, T cell.

considered several possible explanations such as: (a) the limited lineage spectrum of progeny cells may reflect the presence of progenitors with equally limited potential, (b) HSCs are intrinsically heterogeneous in terms of developmental potential, and (c) BM environment is heterogeneous in its ability to support the differentiation of distinct lineages. However, as will be discussed later, these cases seemed quite unlikely. Instead of above ideas, we came to think that the unexpected production of limited cell lineages by HSCs may be explained by assuming the presence of mosaic-like hematopoietic environments that can differently support the "commitment" of early multipotent progenitors to a certain lineage.

We attempted to test this idea by modeling and simulation. For simplicity, granulocytes and monocytes are placed into the myeloid lineage while T and NK cells are placed into the T lineage, consequently all lineages being classified into M, E, T, and B lineages. The clinically observed data for chimerism ratio and detected lineages shown in Figure 2A are replotted in Figure 6A. For cases where the proportion of GPI-APs⁻ clones is between 0.3% and 3% (representing typical size clones), the frequencies of different lineage combinations are shown in Figure 6B.

We assume that a self-renewing HSC is located in a particular location in BM and that uncommitted progenitors derived from this HSC can reach to a certain defined area

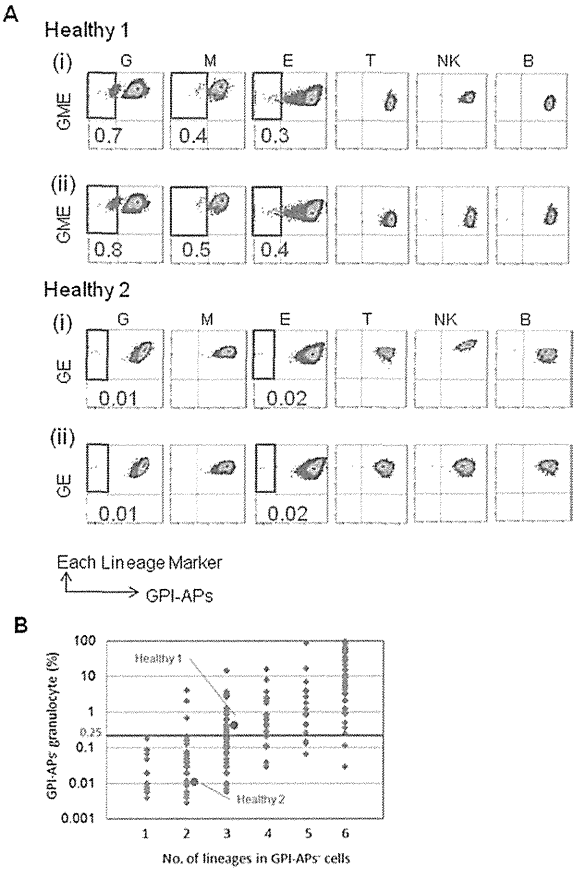

Figure 5. GPI-APs$^-$ cells in healthy individuals. **(A):** Two healthy individuals (healthy 1 and healthy 2) showed GPI-APs$^-$ cells in the same lineage combination pattern at the first sampling (i) and 13 and 7 months after the first sampling (ii), respectively. **(B):** The percentage of GPI-APs$^-$ granulocytes in the two healthy individuals is shown as closed circle in red. ◆, aplastic anemia and myelodysplastic syndrome cases are shown in Figure 2A. Abbreviations: GPI-APs, glycosylphosphatidylinositol-anchored proteins; GMET, Granulocyte, Monocyte, Erythrocyte, T cell.

(Fig. 6C), which we term here the "commitment sphere" (see also Supporting Information Note for detailed information). If the BM microenvironment is mosaic in terms of function in inducing the commitment of progenitors toward a certain lineage, and the size of such mosaic is as large as commitment sphere, then production of progenitors of limited lineages can occur.

In our model, it is critical to determine how the mosaic-like environment is distributed in BM. To this end, we comprehensively examined 112 kinds of mosaic patterns, varying grains of area ratios among commitment areas supporting M, E, B, and T. The strategy to generate the patterns is summarized in the Supporting Information Note. For each mosaic pattern out of 112 variants, we simulated that a single randomly located HSC in certain type of mosaic environment undergoes a certain round of cell division and then undergo commitment according to the place they are located. After commitment, cells further make proliferation and finally terminal differentiation to form mature blood cells. For simplicity, the number of cell division before and after commitment is set as 5 and 5, respectively, in the simulation. We then investigated which cell lineages appeared, counting the number of cells belonging to each lineage. A total of 100 clones were simulated for each mosaic pattern. We found that simulation based on 17 mosaic patterns resulted in histograms similar to the clinical data. Figure 6C shows a representative mosaic among them, and Figure 6D shows the histogram for the results of simulations in which a total of 256 of randomly located HSCs gave rise to hematopoietic colonies in the mosaic pattern shown in Figure 6C, which recapitulate the clinical results (Fig. 6B). We also performed simulations of many virtual HSCs in the same mosaic environment while changing clone size (i.e., changing the cell division times before and after commitment, e.g., 3-3, 4-4, 5-5, 6-6, 7-7, resulting in the change in the size of the commitment sphere and the colony of mature cells). The relationship between clone size and number of lineages in each clone was then plotted in Figure 6E, which looks quite similar to Figure 6A. Thus, these simulations may have provided a reasonable explanation for the observed in vivo findings.

In the simulation, we assumed that T/NK cell progenitors and B cell progenitors are generated in distinct sites. If the induction site for T/NK cell progenitors is assumed to completely overlap or to be included as a part of B cell progenitor induction site (Fig. 7A, 7B), our simulation predicts that "MET"-type clones would hardly be generated (Fig. 7C, 7D), which is not the actual case. Therefore, our in vivo findings together with the results of simulation strongly suggest that T/NK cell progenitors are produced in a different site from the one where B cell progenitors are produced.

Discussion

In this study, by flow cytometrically detecting GPI-APs$^-$ cells in major six blood lineages, we have succeeded in visualizing the dynamics of individual HSCs in BM failure patients. The results strongly suggest that most individual human HSCs only give rise to a limited range of hematopoietic progeny even in regular hematopoiesis.

We thought that we should provide a reasonable explanation for this unexpected finding, that is, the detection of GPI-APs$^-$ cells in the limited lineages over long period. Before we reach to our model, we have considered several possibilities to explain this finding, as briefly mentioned in Result. Here, we will discuss these possibilities, (a), (b), and (c).

(a). One possibility is that the limited lineage spectrum of progeny cells may reflect the presence of progenitors with equally limited potential. Indeed, in contrast to classic models of hematopoiesis, which assume the early segregation of HSCs to myelo-erythroid lineage and lymphoid lineage, some recent revised models of both mouse and human hematopoiesis have proposed that myeloid lineages are also derived from lymphoid branches [21, 22]. However, implications of these models in this study seem unlikely, since, as mentioned earlier, it is clear that most cases represent activities of self-renewing HSCs.

(b). Another simple explanation might be that HSCs are intrinsically heterogeneous in terms of developmental potential. Recent studies have shown such heterogeneity in murine HSCs, some being prone to produce myeloid cells while others to produce lymphoid cells [23–28]. However, it seems quite unlikely that HSCs intrinsically have as many as 16 different subtypes as shown in Supporting Information Table S1.

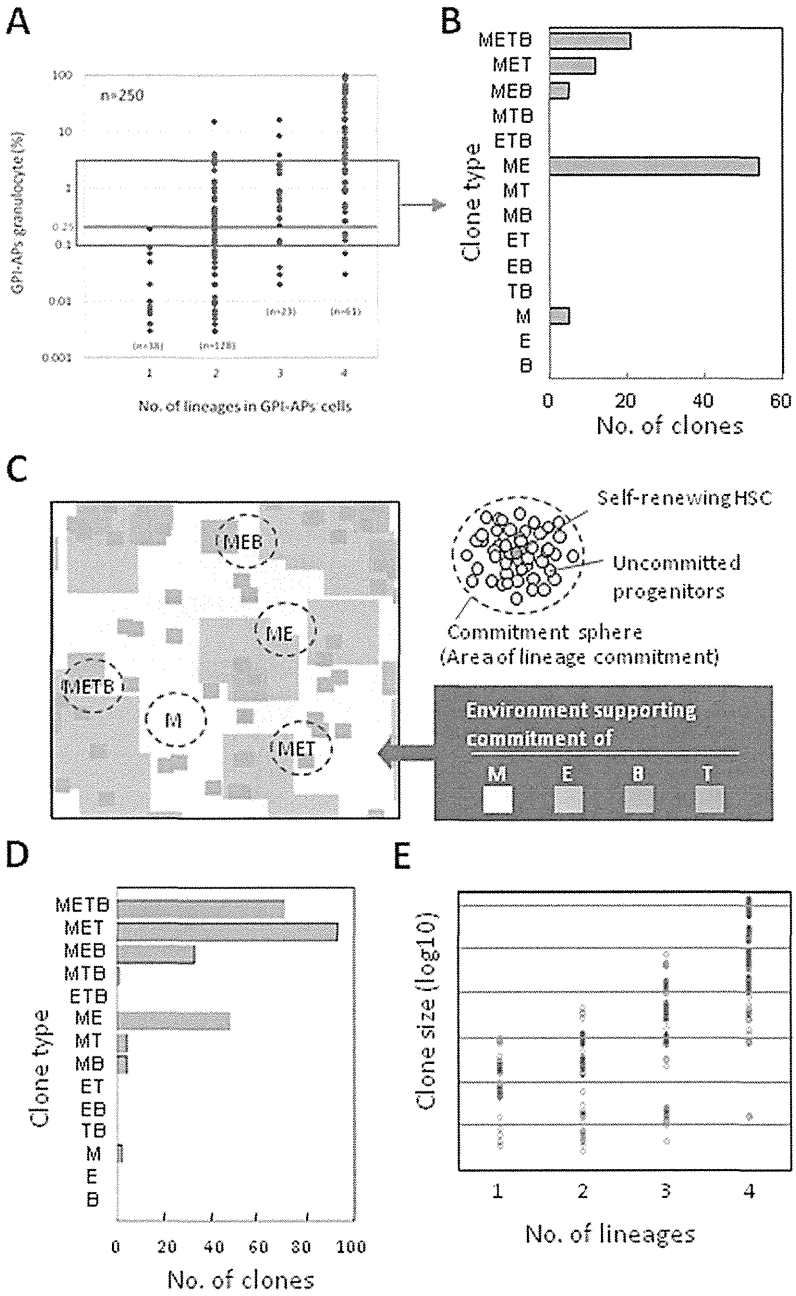

Figure 6. Simulation of hematopoietic stem cell (HSC) differentiation in a model assuming a mosaic environment for the commitment of primitive progenitors recapitulates the clinical observation. **(A):** The percentage of GPI-APs$^-$ granulocytes versus the number of cell lineages in individual patients. Data from Figure 2A were replotted in a setting where granulocytes and monocytes were placed in the myeloid lineage and T and NK cell lineages in the T-cell lineage. A red line for 0.25% stands for the expected value for an average size of a single HSC clone. **(B):** Frequency of clone types among cases where the percentage of GPI-APs$^-$ granulocytes is between 0.3% and 3%. **(C):** A model assuming that the bone marrow microenvironment is heterogeneous in supporting the commitment of progenitors. A certain range where the commitment of progenitors mainly occurs (with a probability of >97%) is termed the commitment sphere (see Supporting Information Note for detailed information). Areas colored by beige, pink, light green, or blue represent the environment supporting commitment only toward M, E, T, or B, respectively. If a HSC happens to reside in a location in which the commitment sphere contains only M and E regions, then this HSC can eventually produce only M and E cells, even if committed progenitors expand enormously and become widely scattered. The depicted simulation goes as follows: a virtual HSC undergoes several cell divisions at fixed intervals while randomly migrating. The uncommitted progenitors then undergo a fate decision based on their ultimate location in the commitment sphere. Committed progenitors can also randomly move around but can proliferate only in the lineage specific supporting environment. After several additional fixed time cell divisions as committed progenitors, cells become mature and lineage restricted. **(D):** One example illustrating the frequency of clone types simulated as shown in (C). A total of 100 virtual HSCs were simulated to form hematopoietic clones, and numbers of the resulting clone types are illustrated (Supporting Information movies 1–5). **(E):** Simulation of individual HCSs for size and number of progeny lineages. The simulation well recapitulated the clinical observations shown in (A). Abbreviation: GPI-APs, glycosylphosphatidylinositol-anchored proteins.

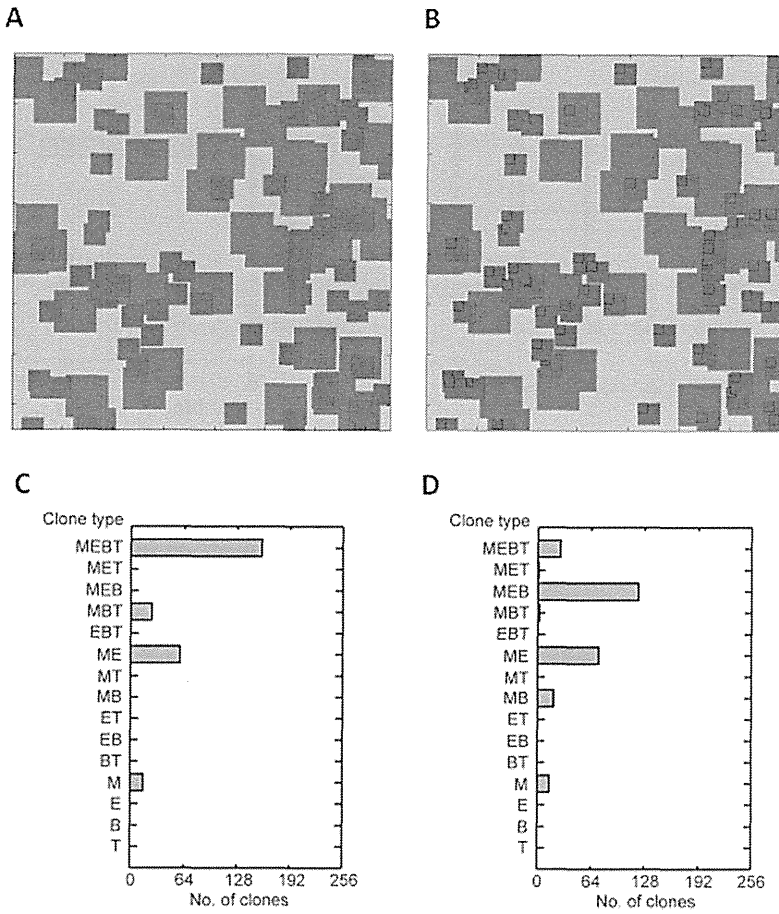

Figure 7. Alternative conditions for induction sites to T and B cell lineages. Illustration of a mosaic pattern in a case where the induction site to the T lineage completely **(A)** or partially **(B)** overlaps with the B lineage (i.e., green area is for both T and B in (A), while blue area is for T and green area is for B in (B)). **(C, D):** Histograms calculated from Panel A (C) or Panel B (D).

(c). It is also possible that the BM environment is heterogeneous in its ability to support the differentiation of distinct lineages. However, this is also quite unlikely. Provided that 400 stem cells contribute to whole hematopoiesis [1, 2] containing 18×10^{11} hematopoietic cells [29] in a total of approximately 1 kg active BM mass [30], the size of the hematopoietic site of one clone maintained by a single HSC in BM could be several cm^3, which may contain on the order of 10^9 hematopoietic cells and a comparable number of stromal cells. It is thus difficult to conceive that such large area contains only limited types of microenvironments.

Thus, we came to think that the above three explanations were quite unlikely. We then came to propose a reasonable model as an explanation of this phenomenon. This model assumes that the microenvironment of BM is mosaic in inducing the commitment of progenitors to distinct lineages. If the size of area where uncommitted progenitors derived from one HSC can reach (commitment sphere in Fig. 6C) is similar to the size of mosaic compartments, production of limited lineage cells can occur. We named our model "mosaic commitment-inducing microenvironment model." This idea on first viewing may sound similar to the idea mentioned above in (c), but clearly different in that our model focuses on only commitment-inducing function of microenvironment and thus the size of mosaic area is much smaller. In this context, our model is also distinct from the classic idea of "hematopoietic inductive microenvironment (HIM)" [31], which is close to the idea mentioned above in (c).

To test whether our model can explain the in vivo findings, we applied a computer simulation approach, and simulations based on this model nicely recapitulated the observed in vivo findings. We emphasize here that we do not claim that our in vivo findings indicate the presence of mosaic commitment-inducing microenvironment in BM, but just propose a novel model that can explain the finding which otherwise is difficult to explain.

We recognize that the issue of whether the dynamics of HSCs observed in this study represents normal hematopoiesis must be critically discussed. Since the stable production of limited lineages was observed in milder cases of AA patients similarly to more severe cases (Fig. 2B), it is likely that these observed dynamics represent normal hematopoiesis. Detection of stable GPI-APs$^-$ clones producing limited lineages in healthy volunteers further supports this notion (Fig. 5).

Nevertheless, here we will make discussion on the issue whether we are making some overestimation or

underestimation in the interpretation of data in AA and MDS cases. Our findings can be summarized as follows: (a) a single HSC gives rise to a limited spectrum of lineage cells and (b) HSCs stably and continuously produce blood cells by years.

As for the finding (a), the possibility could exist that GPI-APs$^-$ HSCs or progenitors have some defect in their migration potential, resulting in a failure to produce the complete spectrum of lineages. Although it is difficult to completely rule out this possibility, so far no published findings are available that support it. Another possible explanation could be that the HSCs in AA or MDS patients are already defective in developmental potential, or that the hematopoietic microenvironments in these patients are disorganized. However, these may not be critical factors, since detection of GPI-APs$^-$ cells of limited lineages was similarly seen in milder cases of AA, and also in healthy volunteers (Figs. 2B, 5). AA and MDS may result from various causes, and it has been supposed that a certain proportion of cases are primarily caused by the impaired function of microenvironment. However, it is likely that in most cases in this study the microenvironment itself is largely normal, because all the patients are bearing GPI-APs$^-$ cells, which is a sign to show that immunological pathophysiology is the main cause of the disease. It can also be noted that most AA patients who undergo allogeneic BM transplantation achieve complete hematologic recovery despite the fact that BM stromal cells are not transplantable [32], indicating that the hematopoietic microenvironments in AA patients are not impaired. Another possibility to be discussed is that the immunological reaction against GPI-APs$^-$ HSCs may affect their blood cell formation, since AA and MDS cases bearing GPI-APs$^-$ cells are thought to be caused by such autoimmune activities. However, such effect cannot be essential, since GPI-APs$^-$ cells are usually out of the target of immune cells, and the autoimmune activities in patients tested in this study have been virtually negligible, judging from the fact that the clone sizes of GPI-APs$^-$ cells in all patients scarcely changed during the observation periods.

We used antibody for CD55, CD59, or CD48 to positively stain GPI-AP expressing cells instead of FLAER that directly stain GPI-APs. In calibration experiments, we have seen that both methods virtually made no difference (data not shown). We note here that our approach could result in the overestimation of the presence of GPI-APs$^-$ cells compared with the FLAER method, since FLAER can cover all GPI-APs. However, such overestimation seems to occur at a very low frequency, and moreover, it will never cause the underestimation for the presence of GPI-APs$^-$ cells.

Finding (b) seems to fit well with the expected dynamics of HSCs. However, this finding could result from an overestimation. Since patients have some BM failure, the total HSC number may be more or less reduced. In such a less competitive situation, it could be that the active HSCs have a better chance to continue hematopoiesis. In addition, GPI-APs$^-$ cells may have some survival advantage over normal blood cells in patients because GPI-APs$^-$ cells may be less sensitive to immunological attacks than GPI-APs$^+$ cells [33]. However, in fact, the combination of GPI-APs$^-$ lineage as well as the proportion of GPI-APs$^-$ cells in PB persisted over a long period as it is, indicating that most of clones do not have an obvious dominance against other clones. It is also important to note that any possible overestimation in HSC longevity does not call into question finding (a).

Conclusion

Finally, it should be discussed whether such heterogeneity as proposed in our model can actually be observed in the BM environment. Heterogeneity of stromal environment has been pointed out in early studies for example based on the findings of preferential generation of erythroid or granulocytic cells in spleen and BM, respectively [31]. A recent study has suggested the presence of a microenvironment that selectively supports B cell development in murine BM [34]. This then leads to the question of how large is the commitment sphere and mosaic fragments of the BM environment? We do not have any data concerning the actual size of the commitment sphere or compartments of mosaic environments, but would suggest that the relative size of these two may be similar to each other. Thus, each piece of the mosaic could be very small, containing only a few stromal cells. We hope that our present report and speculative model will facilitate further study on the distinct niches in BM environment.

Acknowledgments

This study was supported by Grant-in-Aids for Scientific Research from the Ministry of Education, Culture, Sports, Science and Technology of Japan (KAKENHI No. 21390291, http://www.e-rad.go.jp/) and a Grant-in-Aids from the Ministry of Health, Labor and Welfare of Japan. The calculations were performed using the RIKEN Integrated Cluster of Clusters (RICC) facility.

Disclosure of Potential Conflicts of Interest

The authors indicate no potential conflicts of interest.

References

1 Buescher ES, Alling DW, Gallin JI. Use of an X-linked human neutrophil marker to estimate timing of lyonization and size of the dividing stem cell pool. J Clin Invest 1985;76:1581–1584.

2 Traulsen A, Pacheco JM, Luzzatto L et al. Somatic mutations and the hierarchy of hematopoiesis. Bioessays 2010;32:1003–1008.

3 Wang H, Chuhjo T, Yasue S et al. Clinical significance of a minor population of paroxysmal nocturnal hemoglobinuria-type cells in bone marrow failure syndrome. Blood 2002;100:3897–3902.

4 Nishimura J, Inoue N, Wada H et al. A patient with paroxysmal nocturnal hemoglobinuria bearing four independent PIG-A mutant clones. Blood 1997;89:3470–3476.

5 Rosti V, Tremml G, Soares V et al. Murine embryonic stem cells without pig-a gene activity are competent for hematopoiesis with the PNH phenotype but not for clonal expansion. J Clin Invest 1997;100: 1028–1036.

6 Maciejewski JP, Sloand EM, Sato T et al. Impaired hematopoiesis in paroxysmal nocturnal hemoglobinuria/aplastic anemia is not associated with a selective proliferative defect in the glycosylphosphatidylinositol-anchored protein-deficient clone. Blood 1997;89:1173–1181.

7 Araten DJ, Luzzatto L. The mutation rate in PIG-A is normal in patients with paroxysmal nocturnal hemoglobinuria (PNH). Blood 2006;108:734–736.

8 Traulsen A, Pacheco JM, Dingli D. On the origin of multiple mutant clones in paroxysmal nocturnal hemoglobinuria. Stem Cells 2007;25: 3081–3084.

9 Dingli D, Luzzatto L, Pacheco JM. Neutral evolution in paroxysmal nocturnal hemoglobinuria. Proc Natl Acad Sci USA 2008;105: 18496–18500.
10 Hillmen P, Lewis SM, Bessler M et al. Natural history of paroxysmal nocturnal hemoglobinuria. N Engl J Med 1995;333:1253–1258.
11 Sugimori C, Mochizuki K, Qi Z et al. Origin and fate of blood cells deficient in glycosylphosphatidylinositol-anchored protein among patients with bone marrow failure. Br J Haematol 2009;147:102–112.
12 Sugimori C, Chuhjo T, Feng X et al. Minor population of CD55-CD59- blood cells predicts response to immunosuppressive therapy and prognosis in patients with aplastic anemia. Blood 2006;107: 1308–1314.
13 Camitta BM, Thomas ED, Nathan DG et al. A prospective study of androgens and bone marrow transplantation for treatment of severe aplastic anemia. Blood 1979;53:504–514.
14 Bennett JM, Catovsky D, Daniel MT et al. Proposals for the classification of the acute leukaemias. French-American-British (Fab) co-operative Group. Br J Haematol 1976;33:451–458.
15 Araten DJ, Nafa K, Pakdeesuwan K et al. Clonal populations of hematopoietic cells with paroxysmal nocturnal hemoglobinuria genotype and phenotype are present in normal individuals. Proc Natl Acad Sci USA 1999;96:5209–5214.
16 Katagiri T, Qi Z, Ohtake S et al. GPI-anchored protein-deficient T cells in patients with aplastic anemia and low-risk myelodysplastic syndrome: Implications for the immunopathophysiology of bone marrow failure. Eur J Haematol 2011;86:226–236.
17 Mochizuki K, Sugimori C, Qi Z et al. Expansion of donor-derived hematopoietic stem cells with PIGA mutation associated with late graft failure after allogeneic stem cell transplantation. Blood 2008; 112:2160–2162.
18 Mayawala K, Vlachos DG, Edwards JS. Computational modeling reveals molecular details of epidermal growth factor binding. BMC Cell Biol 2005;6:41.
19 Jayawardhana B, Kell DB, Rattray M. Bayesian inference of the sites of perturbations in metabolic pathways via Markov chain Monte Carlo. Bioinformatics 2008;24:1191–1197.
20 Pu JJ, Hu R, Mukhina GL et al. The small population of PIG-A mutant cells in myelodysplastic syndromes do not arise from multipotent hematopoietic stem cells. Haematologica 2012;97:1225–1233.
21 Kawamoto H, Katsura Y. A new paradigm for hematopoietic cell lineages: Revision of the classical concept of the myeloid-lymphoid dichotomy. Trends Immunol 2009;30:193–200.
22 Doulatov S, Notta F, Eppert K et al. Revised map of the human progenitor hierarchy shows the origin of macrophages and dendritic cells in early lymphoid development. Nat Immunol 2010;11:585–593.
23 Muller-Sieburg CE, Cho RH, Karlsson L et al. Myeloid-biased hematopoietic stem cells have extensive self-renewal capacity but generate diminished lymphoid progeny with impaired IL-7 responsiveness. Blood 2004;103:4111–4118.
24 Dykstra B, Kent D, Bowie M et al. Long-term propagation of distinct hematopoietic differentiation programs in vivo. Cell Stem Cell 2007; 1:218–229.
25 Beerman I, Bhattacharya D, Zandi S et al. Functionally distinct hematopoietic stem cells modulate hematopoietic lineage potential during aging by a mechanism of clonal expansion. Proc Natl Acad Sci USA 2010;107:5465–5470.
26 Morita Y, Ema H, Nakauchi H. Heterogeneity and hierarchy within the most primitive hematopoietic stem cell compartment. J Exp Med 2010;207:1173–1182.
27 Cavazzana-Calvo M, Fischer A, Bushman FD et al. Is normal hematopoiesis maintained solely by long-term multipotent stem cells? Blood 2011;117:4420–4424.
28 Nakano T. Hematopoietic stem cells: Generation and manipulation. Trends Immunol 2003;24:589–594.
29 Osgood EE. Number and distribution of human hemic cells. Blood 1954;9:1141–1154.
30 Pichardo JC, Trindade AA, Brindle JM et al. Method for estimating skeletal spongiosa volume and active marrow mass in the adult male and adult female. J Nucl Med 2007;48:1880–1888.
31 Trentin JJ. Determination of bone marrow stem cell differentiation by stromal hemopoietic inductive microenvironments (HIM). Am J Pathol 1971;65:621–628.
32 Awaya N, Rupert K, Bryant E et al. Failure of adult marrow-derived stem cells to generate marrow stroma after successful hematopoietic stem cell transplantation. Exp Hematol 2002;30:937–942.
33 Murakami Y, Kosaka H, Maeda Y et al. Inefficient response of T lymphocytes to glycosylphosphatidylinositol anchor-negative cells: Implications for paroxysmal nocturnal hemoglobinuria. Blood 2002;100: 4116–4122.
34 Kwon KR, Ahn JY, Kim MS et al. Disruption of bis leads to the deterioration of the vascular niche for hematopoietic stem cells. Stem Cells 2010;28:268–278.

See www.StemCells.com for supporting information available online.

Thrombosis Research 132 (2013) e118–e123

Contents lists available at ScienceDirect

Thrombosis Research

journal homepage: www.elsevier.com/locate/thromres

Regular Article

Antithrombin deficiency in three Japanese families: One novel and two reported point mutations in the antithrombin gene

Keiko Maruyama [a], Eriko Morishita [a,b,*], Megumi Karato [c], Tadaaki Kadono [d], Akiko Sekiya [a], Yukie Goto [a], Tomomi Sato [a], Haruka Nomoto [a], Wataru Omi [e], Sachie Tsuzura [f], Hidenori Imai [g], Hidesaku Asakura [b], Shigeki Ohtake [a,b], Shinji Nakao [b]

[a] Department of Clinical Laboratory Science, Kanazawa University Graduate School of Medical Science, Kanazawa, Japan
[b] Department of Hematology, Kanazawa University Hospital, Kanazawa, Japan
[c] Toyama Prefectural Arakawa Health and Welfare Center, Toyama, Japan
[d] Kanazawa Municipal Hospital, Kanazawa, Japan
[e] Department of Cardiovascular Medicine, Organization Kanazawa Medical Center, Kanazawa, Japan
[f] Department of Diabetes and Endocrine Medicine, Chikamori Hospital, Kochi, Japan
[g] Department of Hematology, Juntendo University Urayasu Hospital, Chiba, Japan

ARTICLE INFO

Article history:
Received 25 January 2013
Received in revised form 25 May 2013
Accepted 2 June 2013
Available online 25 June 2013

Keywords:
Antithrombin deficiency
factor Xa inhibition activity assay
thrombin inhibition activity assay

ABSTRACT

Introduction: Inherited antithrombin (AT) deficiency is associated with a predisposition to familial venous thromboembolic disease. We analyzed the AT gene in three unrelated patients with an AT deficiency who developed thrombosis.
Materials and Methods: We analyzed the *SERPINC1* gene in three patients. Additionally, we expressed the three mutants in the COS-1 cells and compared their secretion rates and levels of AT activity with those of the wild-type (WT).
Results: We identified three distinct heterozygous mutations of c.2534C>T: p.56Arginine → Cysteine (R56C), c.13398C>A: p.459Alanine → Aspartic acid (A459D) and c.2703C>G: p.112 Proline → Arginine (P112R). In the *in vitro* expression experiments, the AT antigen levels in the conditioned media (CM) of the R56C mutant were nearly equal to those of WT. In contrast, the AT antigen levels in the CM of the A459D and P112R mutants were significantly decreased. The AT activity of R56C was decreased in association with a shorter incubation time in a FXa inhibition assay and a thrombin inhibition-based activity test. However, the AT activity of R56C was comparable to that of WT when the incubation time was increased.
Conclusions: We concluded that the R56C mutant is responsible for type II HBS deficiency. We considered that the A459D and P112R mutants can be classified as belonging to the type I AT deficiency.

Introduction

Antithrombin (AT) is a plasma serine protease inhibitor (serpin) that inactivates a number of proteases in the coagulation cascade, particularly thrombin and factor Xa (FXa) [1]. The human AT gene measures 13.5 kb in length, comprises seven exons and six introns and is located on human chromosome 1 at q23.1-23.9 [2]. Plasma AT is synthesized by hepatocytes as a 464 amino acid precursor with a 32 amino acid single peptide that is cleaved off before secretion as a 432 amino acid mature inhibitor into the plasma. It is a single chain glycoprotein with a molecular weight of approximately 58 kDa [3].

AT is a globular protein composed of three β-sheets (A, B and C), nine α-helices and a reactive center loop (RCL). The RCL protrudes above the core of the serpin molecule and has a sequence of amino acids at the reactive center that is complementary to binding pockets in the active sites of target proteases [4,5]. The AT activity is accelerated approximately 1,000-fold by the binding of heparin to arginine (Arg) residues in the D-helix of the AT protein, which occurs via two different mechanisms [6,7]. A conformational change induced by binding to a specific pentasaccharide sequence within heparin allosterically activates the inhibitor, thereby increasing the inhibition rate. Moreover, a bridging effect, by which heparin brings AT and the protease into a ternary complex, further increases this rate [8]. The individual contributions of these two mechanisms to the heparin-related acceleration of AT

Abbreviations: AT, Antithrombin; serpin, Serine protease inhibitor; FXa, Factor Xa; RCL, Reactive center loop; Arg, Arginine; Lys, Lysine; VTE, Venous thromboembolism; type II RS, Type II reactive site defects; type II HBS, Type II heparin binding site defects; type II PE, Type II with pleiotropic defects; cDNA, Complementary DNA; WT, Wild-type; COS-1 cells, Green monkey kidney cells; Cys, Cysteine; Pro, Proline; Ala, Alanine; Asp, Aspartic acid; PMSF, Phenylmethyl sulfonylfluoride; ELISA, Enzyme-linked immunosorbent assay; RFLP, Restriction fragment length polymorphism analysis; CM, Conditioned media; CL, Cell lysates; PE, Pulmonary thromboembolism; DVT, Deep vein thrombosis.

* Corresponding author at: Department of Clinical Laboratory Sciences, Graduate School of Medical Science, Kanazawa University, 5-11-80 Kodatuno Kanazawa, Ishikawa 920-0942, Japan. Tel./fax: +81 76 265 2606.
E-mail address: eriko86@staff.kanazawa-u.ac.jp (E. Morishita).

0049-3848/$ – see front matter © 2013 Published by Elsevier Ltd.
http://dx.doi.org/10.1016/j.thromres.2013.06.001

inhibition vary for different proteases, the conformational change being of major importance for FXa and IXa, and the bridging effect dominating for thrombin [9]. The X-ray structures of AT and its complex with a synthetic variant of the heparin pentasaccharide indicate that this change involves the elongation of the A- and D-helices, the formation of a new short P-helix at the base of the D-helix and the contraction of the A-sheet. These changes lead to a higher level of accessibility of the reactive bond and exposure of exosites surrounding the loop, thus promoting the binding of target proteases [10]. The region of AT to which the heparin pentasaccharide binds with high affinity and specificity consists primarily of positively charged lysines and arginines within the A- and D-helices and the N-terminal region, including Lys43, Arg45, Arg78, Arg79, Lys146, Lys157 and Arg161 [11]. Lys43, Arg45, Arg78 and Arg79 make lesser contributions to the binding affinity since mutations of any one of these residues result in the loss of binding energy, which, in most cases, approximates the loss of a single ionic interaction. In contrast, Lys146, Lys157 and Arg161 represent binding hotspots since mutations of any one of these residues cause major losses in binding energy that are much greater than would be expected from the loss of a single ionic interaction [12].

An inherited AT deficiency is an autosomal dominant thrombotic disorder associated with a 1.7–4.0% overall annual incidence of venous thromboembolism (VTE) [13,14]. The two primary AT deficiency phenotypes are defined based on the plasma levels of functional and antigenic AT. Type I AT deficiency is characterized by equally low functional and antigenic AT levels, whereas type II deficiency covers all variants with reduced functional but normal AT levels. Depending on the localization of the mutation, type II deficiency is further subdivided into three groups: i) type II reactive site defects (type II RS) are characterized by a low serine protease reactivity in both the presence and absence of heparin; ii) type II heparin binding site defects (type II HBS) are associated with an impaired heparin binding capacity, but normal serine protease reactivity in the absence of heparin; and iii) type II defects associated with pleiotropic defects (type II PE) [15,16]. In type II PE deficiency, the amino acid substitutions affect the highly conserved C-terminal hinge region (strand 1C-5B) of AT, resulting in a decreased circulating concentration of abnormal AT molecules, with impaired heparin binding and serine protease inhibition capacity.

In this study, we evaluated the AT deficiency in three Japanese patients and identified three distinct mutations, including one novel mutation in the AT gene. Additionally, we expressed the three mutants in green monkey kidney cells (COS-1 cells) and compared their secretion rates and levels of AT activity with those of the wild-type (WT) gene product.

Materials and Methods

Materials

The pcDNA3.1/AT expression plasmid containing the full-length AT complementary DNA (cDNA) was kindly provided by Dr. Tsuneo Imanaka (Toyama University, Japan). The Big Dye Terminator v3.1 Cycle Sequencing Kit was purchased from Applied Biosystems Japan, Ltd. Dulbecco's modified Eagle medium (DMEM) was obtained from Nissui Seiyaku (Tokyo, Japan), and fetal bovine serum (FBS) was purchased from Serum Source International, Inc. (Charlotte, NC). The TaKaRa Ligation kit Ver. 2 was obtained from TaKaRa Bio, Inc. (Ohtsu, Japan). HilyMax Transfection Reagent was purchased from DOJINDO (Kumamoto, Japan). Amicon ultra was obtained from Nihon Millipore, Inc. (Tokyo, Japan). A Matched-Pair Antibody Set for the enzyme-linked immunosorbent assay (ELISA) of human AT antigens was purchased from Affinity Biologicals, Inc. (Ontario, Canada). Thrombin was purchased from Sigma Aldrich (St Louis, MO), and heparin was purchased from Novo Industry (Copenhagen, Denmark). The FXa and chromogenic substrates S2238 and S2222 were provided by Sekisui Medical (Tokyo, Japan).

Sample Preparation

Ethical approval for the study was obtained from the Ethics Committee of Kanazawa University School of Medicine, Japan. After obtaining informed consent, venous blood samples were collected from patients with AT deficiency in a 1:10 volume of 3.13% (wt/vol) trisodium citrate. The plasma was separated via centrifugation at × 2,000 g for 20 minutes, and genomic DNA was isolated from peripheral blood leukocytes.

Identification of Abnormalities in the Patients' AT Genes

All seven exons, including the splice junctions of the AT gene, were amplified via PCR using the primer sets listed in Table 1. The DNA was subjected to the following PCR conditions: 30 cycles of denaturation at 94 °C for 60 seconds, annealing at 55 ~ 60 °C for 30 seconds and extension at 70 °C for 30 seconds. The obtained PCR product was directly sequenced using a Big Dye Terminator v3.1 Cycle Sequencing Kit and an ABI PRISM 310 genetic analyzer. The initial Met residue was denoted as amino acid +1.

Site-Directed Mutagenesis of AT

The Arg56 → Cysteine (Cys) (R56C), Proline (Pro) 112 → Arg (P112R) and Alanine (Ala) 459 → Aspartic acid (Asp) (A459D) mutations were introduced into the full length AT cDNA in the pcDNA3.1(+) plasmid using the TaKaRa Ligation kit Ver.2. The primers used for mutagenesis are listed in Table 2. The AT cDNA was sequenced to confirm the presence of a mutation.

Transient Expression of Recombinant AT

COS-1 cells were grown in DMEM supplemented with 10% FBS at 37 °C in 5% CO_2. The cells were cultured in 60-mm dishes and transiently transfected using HilyMax Transfection Reagent. Following incubation in FBS-free DMEM for 24 hours, the cells were lysed in buffer comprising 50 mmol/l Tris–HCl (pH 7.5), 1% BSA, 2 mmol/l of EDTA, 1% Triton X-100, 0.1 mol/l of NaCl, 100 U/ml of aprotinin, 1 μg/ml of leupeptin, 1 μg/ml of pepstain and 200 mmol/l of phenylmethyl sulfonylfluoride (PMSF). The conditioned medium (CM) was concentrated with Amicon ultra. The recombinant proteins were not purified. The following experiments were performed using the CM.

AT Antigen and Activity Measurements in the Conditioned Medium (CM) and Cell Lysates (CL)

The antigen levels of the recombinant AT molecules were measured using ELISA with a Matched-Pair Antibody Set for ELISA of the human AT antigen. The AT activity levels were measured using the FXa inhibition activity assay and the thrombin inhibition activity assay with the CM containing each recombinant AT protein. The reaction of recombinant AT with 4 U/ml of thrombin or 3.55 nkat/ml of FXa was studied at 37 °C in the presence of 60 IU/l of heparin. Recombinant AT was incubated with thrombin in Tris buffer (50 mmol/l of Tris–HCl, 100 mmol/l of NaCl, pH 7.4). At different

Table 1
Oligonucleotide primers used for the amplification of the *SERPINC1* gene.

Exon	Forward primer (5' → 3')	Reverse primer (5' → 3')
1	TCAGCCTTTGACCTCAGTTC	AGGTCACAAAACCCATGAGG
2	GGCAGTGGGGCTAGGGGTT	TTGAGGAATCATTGGACTTGGG
3a	ACCACCCATGTTAACTAGGC	AGCAGCAAAGCAGTGTGAAT
3b	TAGCACAGGTGAGTAGGTTTATT	GAAGAGCAAGAGGAAGTCCCT
4	CAATAACTATCCTCCTATGAATG	CTTTCTCCAACTCTTCCACTTTT
5	AGCCAACTTTCTCCCATCTC	CAGAAGAGGTAGTGGGAGGG
6	TCTGTGGATGATTTACCTGC	TTCACAAACCAAAAATAGGA

Table 2
Oligonucleotides used for site-directed mutagenesis.

Mutation	Forward primer(5' → 3')	Reverse primer(5' → 3')
R56C	CATTTACTGCTCCCCGGAGAAG	CATGGGATTCATGGGAATGTCCC
A459D	GCAGAGTAGACAACCCTTGTGTTAAG	GCAGAGTAGACAACCCTTGTGTTAAG
P112R	CATTTTCCTGTCACGCCTGAGTATC	TTATCATTGTCATTCTTGGAATCTGCCAG

The underlined letters indicate the mismatches.

times, the chromogenic substrates S2238 and S2222 were added to the reaction mixture, and the absorbance was read at 405 nm to determine the residual thrombin or FXa activity. The specific activity of each recombinant AT mutant was calculated as a percentage of the wild-type AT activity.

Statistical Analysis

Between group comparisons were conducted using paired or unpaired t-tests for normally distributed data. All data are presented as the mean ± standard error of the mean. For all statistical analyses, a value of $p < 0.05$ was considered to be statistically significant.

Results

Cases

Patient 1 was a 65-year-old Japanese female who developed pulmonary thromboembolism (PE). Her level of plasma AT antigens was 91%. The FXa inhibition activity assay (Testzym S ATIII kit, Sekisui Medical) also provided a normal value; however, a decreased AT activity level (approximately 59%) was observed on a thrombin inhibition-based activity test. Her family members did not have a history of thrombosis.

Patient 2 was a 20-year-old Japanese female who developed deep vein thrombosis (DVT) at 14 years of age. Her levels of plasma AT activity and antigens were 23% and 49%, respectively. The AT activity and antigen levels of the proband's mother were 46% and 69%, respectively. Her father had no abnormalities. A family history revealed that her maternal grandmother had developed thrombosis.

Patient 3 was a 39-year-old Japanese female. On a preoperative examination for resection of ovarian cancer, her levels of plasma AT activity and AT antigens were 53% and 54%, respectively. Her father had a history of DVT, and his level of AT activity was 49%.

The antigen and activity levels of other anticoagulants are within the reference ranges in all three patients. In addition, the patients had negative tests for antiphospholipid antibodies and lupus anticoagulant. Moreover, they had no other risk factors (such as cancer, pregnancy or drugs), with the exception that patient 1 had hyperlipidemia and hypertension and patient 3 had ovarian cancer.

Identification of Three AT Mutations

We analyzed the AT gene in these three unrelated Japanese patients with AT deficiencies using PCR-mediated direct sequencing and identified three distinct mutations (Fig. 1). Patient 1 carried a C to T mutation at nucleotide 2534 of the AT gene, which changed the codon for Arg56 (CGC) to Cys (TGC). Patient 2 harbored a C to A mutation at nucleotide 13398 of the AT gene, which changed the codon for Ala459 (GCC) to Asp (GAC). Her mother also carried this mutation. Patient 3 carried a C to G mutation at nucleotide 2703 of the AT gene, which changed the codon for Pro112 (CCC) to Arg (CGC). Her father and daughter also carried this mutation. These mutations included two previously reported mutations (A459D and R56C) and one novel mutation (P112R), all of which were in the heterozygous state. According to the criterion that the amino terminal of mature AT denotes amino acid +1, these mutations are represented as A427D, R24C and P80R.

AT Antigen and Activity Measurements in the Conditioned Medium (CM) and Cell Lysates (CL)

The AT antigen levels in the CL harboring AT-R56C, A459D and P80R were comparable to that of AT-WT (R56C: 127 ± 6%, A459D: 170 ± 23% and P80R: 113 ± 5%, Fig. 2A). In the CM, the AT-R56C antigen level was nearly equal to that of the AT-WT cells (107 ± 6%, Fig. 2A). On the other hand, the AT antigen level in the CM of AT-A459D and P112R was significantly decreased (A459D: 27 ± 3%, P112R: 18 ± 9%, Fig. 2A). The activity of AT-R56C was decreased compared to that of AT-WT when the incubation time was three minutes in the FXa inhibition assay (71 ± 3%, Fig. 2B). Interestingly, the activity of AT-R56C was further decreased when the incubation time was reduced to 30 seconds in the FXa inhibition assay (31 ± 14%, Fig. 2B). In addition, the activity of AT-R56C was reduced in a thrombin inhibition-based activity test (45 ± 12%, Fig. 2B). However, the activity of AT-R56C was comparable to that of AT-WT when the incubation time was increased to five minutes (86 ± 16%, Fig. 2B). The same results were observed when we measured the levels using the patient's plasma (FXa inhibition activity assay: 30 s: 50 ± 3%, 3 min: 113 ± 3%, thrombin inhibition-based activity test: 30 s: 60 ± 3%, 5 min: 114 ± 3%, Fig. 3). Therefore, the difference between AT-R56C and AT-WT was maximal at a short incubation time (30 s) and became less apparent as the incubation time increased.

Discussion

We investigated three cases of AT deficiency and discovered three heterozygous mutations in exons 2 and 6 of the AT gene. Patient 1 had a previously reported mutation (c.2534C>T), resulting in R56C as AT Rouen IV. Patient 2 had a previously reported mutation (c.13398C>A), resulting in A459D. Patient 3 had a novel mutation (c.2703C>G), resulting in P112R. In the *in vitro* expression experiments, we found that the R56C mutant was associated with the sensitivity of the FXa inhibition assay and a thrombin inhibition-based activity test. The A459D and P112R mutants were considered to lead to impaired secretion and to be degraded intracellularly, resulting in type I AT deficiency.

Patient 1 was a heterozygous carrier of the R56C mutation and developed PE. Borg et al. previously reported a patient who was a heterozygous carrier of this mutation (AT Rouen IV). They showed that the patient's plasma had a decreased affinity for heparin-sepharose and a decreased heparin-induced inhibitory activity [17]. Schedin-Weiss et al. showed that a mutation of Arg56 to Ala reduced the affinity for the pentasaccharide ~40-fold and that Arg56 is of appreciable importance in the second binding step because it stabilizes the activated state of the inhibitor by forming intramolecular interactions with Glu145 and Asp149, which are located in the pentasaccharide-induced P-helix [18]. The P-helix is formed as an essential component of the pentasaccharide-induced conformational change [19]. Its creation serves primarily to position the pivotal Lys146 residue, which thus far appears to provide the greatest contribution to the pentasaccharide-induced conformational change [20]. The losses of ionic and nonionic interactions with the pentasaccharide and the resulting loss in overall affinity observed in the mutation of Arg56 are therefore most likely due to alterations of interactions involving Lys146.

The patient's plasma AT activity was normal in the routine FXa inhibition activity assay, although a decreased AT activity level (approximately 59%) was observed in a thrombin inhibition-based

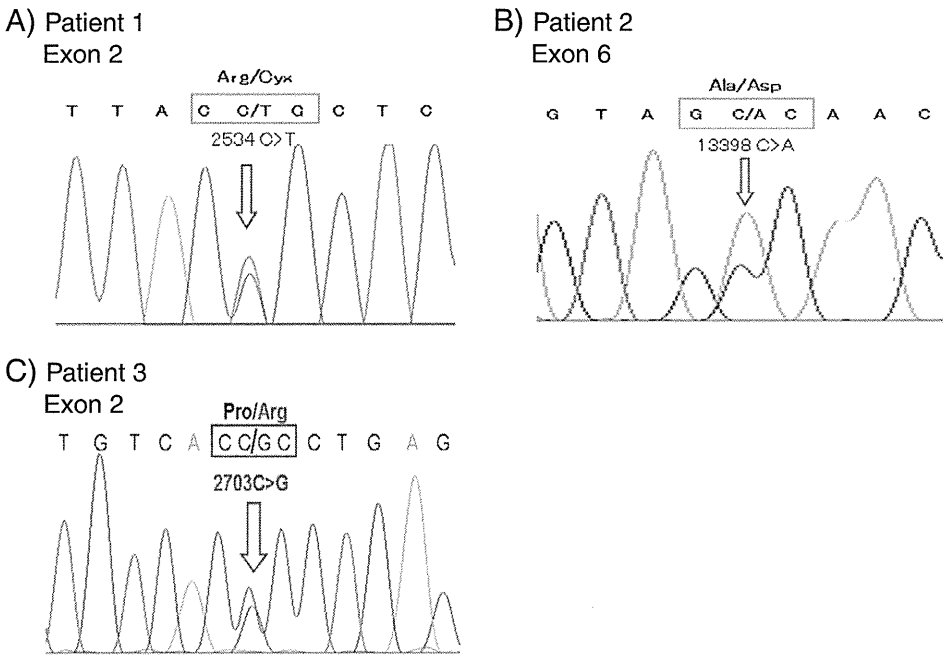

Fig. 1. Sequencing analysis of the *SERPINC1* gene in the probands of patient 1 (A), patient 2 (B) and patient 3 (C). Electropherograms show the missense mutation (arrow) and surrounding nucleotides.

activity test. Using recombinant proteins and the patient's plasma, we showed that the difference between the R56C and WT activity was maximal at a short incubation time and became less apparent as the incubation time increased in both the FXa inhibition assay and thrombin inhibition-based activity test. A previous report showed that AT Cambridge II (p.Ala416Ser), AT Denver (p.Ser426Asp) and AT Stockholm (p.Gly424Asp) have been detected in assays using human and bovine thrombin, while normal levels are seen in FXa-based assays [21,22]. Cooper et al. reported that, in their study, subjects with HBS defects (AT Basel, p.Pro73Leu) exhibited fewer defects at shorter incubation times when assessed according to the FXa, while the defects were reliably detected using FXa with plasma dilution and incubation in excess of four minutes in a Coamatic AT assay [22]. Harper et al. showed that the sensitivity of bovine thrombin-based AT assays to type IIHBS defects is significantly improved when the incubation time of the samples diluted with thrombin is reduced to 30 seconds or less [23]. We

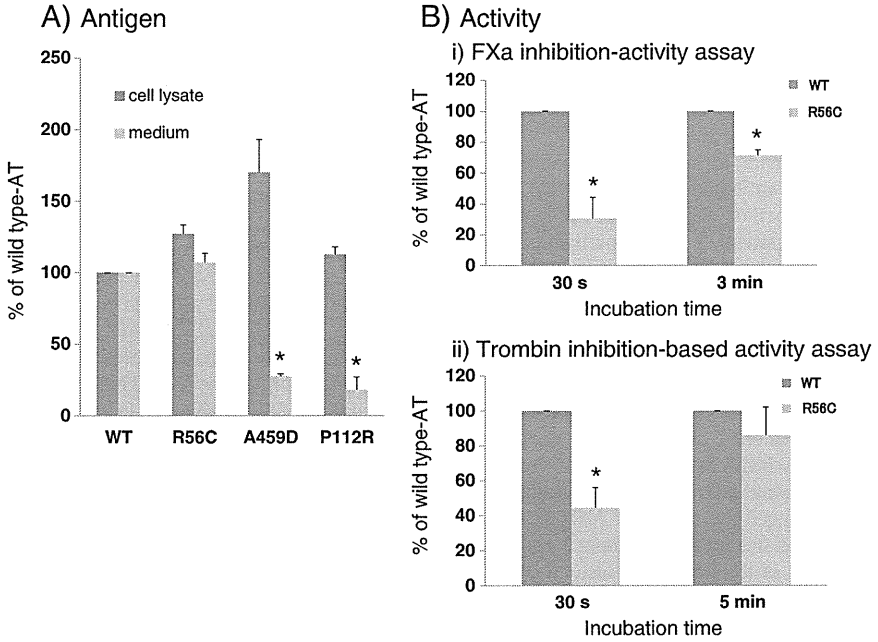

Fig. 2. The levels of AT antigens (A) and activity (B, C) of recombinant AT produced by COS-1 cells transfected with wild-type (WT) and mutant AT expression vectors. (A) The relative antigen levels in the cell lysate and media measured using ELISA are shown. The AT activity of CM contained in each recombinant protein was measured using a factor Xa inhibition activity assay (B) and thrombin inhibition activity assay (C). All values represent the mean ± SD of three experiments. $^{*}p < 0.05$ compared with the antigen or activity levels of WT.

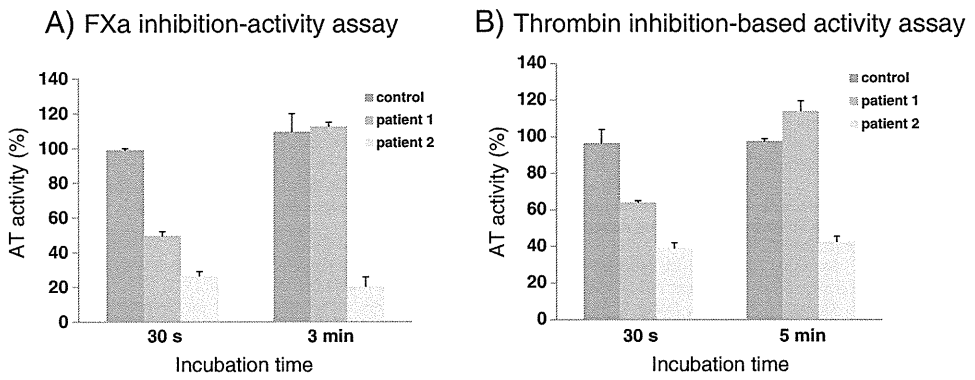

Fig. 3. The levels of AT activity in the patients' plasma. The AT activity levels in the patients' plasma were measured using a factor Xa inhibition activity assay (A) and thrombin inhibition activity assay (B).

considered that the R56C mutation might therefore contribute to the sensitivity of the FXa inhibition assay and the thrombin inhibition-based activity test.

Patient 2 was a heterozygous carrier of the A459D mutation and developed DVT. Millar et al. previously reported that the A459D mutation is associated with type I AT deficiency [24]. The A459D mutant influences the tertiary structure of the molecule by disturbing the alignment of sheets 4B and 5B, which are important for the stability of the mutant AT protein [25]. In a recent paper, the structure of a domain swapped with an antitrypsin trimer revealed that the C-terminal region of the molecule formed the domain swap [26]. Serpin polymerization led to the accumulation of hyperstable polymers in the endoplasmic reticulum of secretory cells. In our study, the AT antigen level in the CM of the A459D mutant was decreased in the ELISA. Therefore, the A459D mutation may be associated with type I AT deficiency.

Patient 3 was heterozygous for a P112R mutation. She had no history of thrombosis. However, her father also carried this mutation and had a history of DVT. This mutation is a novel mutation. Pro112 is located in the shutter region. The shutter region of the serpins is vital for the stability of serpins, primarily due to the importance of the region in controlling the mobility of the A β-sheet strands, which in turn, is pivotal to the function and stability of serpin [27]. Previous reports have shown that Pro112 is changed to Thr [28] and Ser [29]. P112T is associated with a type I deficiency state manifesting as reduced synthesis of AT [28]. In contrast, the abnormal AT purified from P112S carriers is an inactive disulfide-linked dimer of mutant AT [29]. Yamasaki M et al. reported that this AT mutant polymer is mediated by a domain swap including both strands 4 and 5A, not by loop sheet polymerization [30,31] In addition, Martínez-Martínez I et al. reported that mutations inducing conformational instability in AT (such as F271S and R425del) initiate protein polymerization under mild stress that sequestrates WT functional monomers, resulting in the gain of a new prothrombotic function, which is particularly relevant for intracellular AT [32]. We showed that the AT antigen level in the CM of P112R was significantly decreased in an ELISA. Therefore, the P112R mutation may be responsible for type I AT deficiency, as well as P112T, resulting in replacement by a positively charged amino acid. Furthermore, Pro112 forms a hydrogen bond to Ser116. The P112R mutant is conformationally unstable because it cannot form a hydrogen bond with Ser116. In this study, we were unable to investigate whether disulfide-linked dimers were present in the plasma of the patient and the CM of the P112R and A459D mutants. We are planning a further examination.

In conclusion, our data showed that heterozygous mutations of c.2534C>T (R56C), c.13398C>A (A459D) and c.2703C>G (P112R) in the AT gene caused AT deficiency in three unrelated Japanese pedigrees. We assumed that the R56C mutation may be associated with the binding of heparin and contributes to the sensitivity of the FXa inhibition assay and thrombin inhibition-based activity test. Our findings suggest that the A459D and P112R mutants are responsible for type I AT deficiency.

Conflict of Interest Statement

None declared.

Acknowledgments

The authors would like to thank Dr. Tsuneo Imanaka for providing the pcDNA3.1/AT expression plasmid and Sekisui Medical (Tokyo, Japan) for providing factor Xa and the chromogenic substrate. This study was supported in part by a Grant-in-Aid for Scientific Research from the Ministry of Education, Science, Sports and Culture of Japan (to E.M.) and by research grants from Kanazawa University, Kanazawa (to A.S.).

References

[1] Rosenberg R, Damus P. Purification and mechanism of action of human antithrombin-heparin cofactor. J Biol Chem 1973;248:6490–505.
[2] Olds RJ, Lane DA, Chowdhury V, De Stefano V, Leone G, Thein SL. Complete nucleotide sequence of the antithrombin gene: Evidence for homologous recombination causing thrombophilia. Biochemistry 1993;32:4216–24.
[3] Jin L, Abrahams JP, Skinner R, Petitou M, Pike RN, Carrell RW. The anticoagulant activation of antithrombin by heparin. Proc Natl Acad Sci U S A 1997;94:14683–8.
[4] Stein PE, Carrell RW. What do dysfunctional serpins tell us about molecular mobility and diseases? Nat Struct Biol 1995;2:96–113.
[5] Petitou M, Duchaussoy P, Herbert JM, Duc G, El Hajji M, Branellec JF, et al. The synthetic pentasaccharide fondaparinux: first in the class of antithrombotic agents that selectively inhibit coagulation factor Xa. Semin Thromb Hemost 2002;28:393–402.
[6] Huntington JA, Olson ST, Fan B, Gettins PG. Mechanism of heparin activation of antithrombin: evidence for reactive center loop preinsertion with expulsion upon heparin binding. Biochemistry 1996;35:8495–503.
[7] Yang L, Manithody C, Qureshi SH, Rezaie AR. Contribution of exosite occupancy by heparin to the regulation of coagulation proteases by antithrombin. Thromb Haemost 2010;103:277–83.
[8] Olson ST, Swanson R, Patston PA, Björk I. Apparent formation of sodium dodecyl sulfate-stable complexes between serpins and 3,4-dichloroisocoumarin-inactivated proteinases is due to regeneration of active proteinase from the inactivated enzyme. J Biol Chem 1997;272:13338–42.
[9] Desai UR, Petitou M, Björk I, Olson ST. Mechanism of heparin activation of antithrombin: evidence for an induced-fit model of allosteric activation involving two interaction subsites. Biochemistry 1998;37:13033–41.
[10] Chuang YJ, Swanson R, Raja SM, Olson ST. Heparin enhances the specificity of antithrombin for thrombin and factor Xa independent of the reactive center loop sequence. Evidence for an exosite determinant of factor Xa specificity in heparin-activated antithrombin. J Biol Chem 2001;276:14961–71.
[11] Olson ST, Björk I, Bock SC. Identification of critical molecular interactions mediating heparin activation of antithrombin: implications for the design of improved heparin anticoagulants. Trends Cardiovasc Med 2002;12:198–205.
[12] Olson ST, Richard B, Izaguirre G, Schedin-Weiss S, Gettins PG. Molecular mechanisms of antithrombin-heparin regulation of blood clotting proteinases. A paradigm for understanding proteinase regulation by serpin family protein proteinase inhibitors. Biochimie 2010;92:1587–96.

[13] Mahmoodi BK, Brouwer JL, Ten Kate MK, Lijfering WM, Veeger NJ, Mulder AB, et al. A prospective cohort study on the absolute risks of venous thromboembolism and predictive value of screening asymptomatic relatives of patients with hereditary deficiencies of protein S, protein C or antithrombin. J Thromb Haemost 2010;8:1193–200.
[14] Sekiya A, Morishita E, Karato M, Maruyama K, Shimogawara I, Omote M, et al. Two case reports of inherited antithrombin deficiency: a novel frameshift mutation and a large deletion including all seven exons detected using two methods. Int J Hematol 2011;93:216–9.
[15] Picard V, Nowak-Göttl U, Biron-Andreani C, Fouassier M, Frere C, Goualt-Heilman M, et al. Molecular bases of antithrombin deficiency: twenty-two novel mutations in the antithrombin gene. Hum Mutat 2006;27:600.
[16] Luxembourg B, Delev D, Geisen C, Spannagl M, Krause M, Miesbach W, et al. Molecular basis of antithrombin deficiency. Thromb Haemost 2011;105:635–46.
[17] Borg JY, Brennan SO, Carrell RW, George P, Perry DJ, Shaw J. Antithrombin Rouen-IV 24 Arg—Cys. The amino-terminal contribution to heparin binding. FEBS Lett 1990;266:163–6.
[18] Schedin-Weiss S, Desai UR, Bock SC, Olson ST, Björk I. Roles of N-terminal region residues Lys11, Arg13, and Arg24 of antithrombin in heparin recognition and in promotion and stabilization of the heparin-induced conformational change. Biochemistry 2004;43:675–83.
[19] Skinner R, Abrahams JP, Whisstock JC, Lesk AM, Carrell RW, Wardell MR. The 2.6 A structure of antithrombin indicates a conformational change at the heparin binding site. J Mol Biol 1997;266:601–9.
[20] Arocas V, Bock SC, Raja S, Olson ST, Bjork I. Lysine 114 of antithrombin is of crucial importance for the affinity and kinetics of heparin pentasaccharide binding. Biol Chem 2001;276:43809–17.
[21] Ungerstedt JS, Schulman S, Egberg N, Antovic J, Blombäck N. Discrepancy between antithrombin activity methods revealed in Antithrombin Stockholm: do factor Xa-based methods overestimate antithrombin activity in some patients? Blood 2002;99:2271–2.
[22] Cooper PC, Coath F, Daly ME, Makris M. The phenotypic and genetic assessment of antithrombin deficiency. Int J Lab Hematol 2011;33:227–37.
[23] Harper PL, Daly M, Price J, Edgar PF, Carrell RW. Screening for heparin binding variants of antithrombin. J Clin Pathol 1991;44:477–9.
[24] Millar DS, Lopez A, White D, Abraham G, Laursen B, Holding S, et al. Screening for mutations in the antithrombin III gene causing recurrent venous thrombosis by single-strand conformation polymorphism analysis. Hum Mutat 1993;2:324–6.
[25] Jochmans K, Lissens W, Yin T, Michiels JJ, van der Luit L, Peerlinck K, et al. Molecular basis for type 1 antithrombin deficiency: identification of two novel point mutations and evidence for a de novo splice site mutation. Blood 1994;84:3742–8.
[26] Yamasaki M, Sendall TJ, Pearce MC, Whisstock JC, Huntington JA. Molecular basis of α1-antitrypsin deficiency revealed by the structure of a domain-swapped trimer. EMBO Rep 2011;12:1011–7.
[27] Stein PE, Carrell RW. What do dysfunctional serpins tell us about molecular mobility and disease? Nat Struct Biol 1995;2:96–113.
[28] Millar DS, Wacey AI, Ribando J, Melissari E, Laursen B, Woods P, et al. Three novel missense mutations in the antithrombin III (AT3) gene causing recurrent venous thrombosis. Hum Genet 1994;94:509–12.
[29] Corral J, Huntington JA, González-Conejero R, Mushunje A, Navarro M, Marco P, et al. Mutations in the shutter region of antithrombin result in formation of disulfide-linked dimers and severe venous thrombosis. J Thromb Haemost 2004;2:931–9.
[30] Yamasaki M, Li W, Johnson DJ, Huntington JA. Crystal structure of a stable dimer reveals the molecular basis of serpin polymerization. Nature 2008;455:1255–8.
[31] Yamasaki M, Sendall TJ, Harris LE, Lewis GM, Huntington JA. Loop-sheet mechanism of serpin polymerization tested by reactive center loop mutations. J Biol Chem 2010;285:30752–8.
[32] Martínez-Martínez I, Navarro-Fernández J, Aguila S, Miñano A, Bohdan N, De La Morena-Barrio ME, et al. The infective polymerization of conformationally unstable antithrombin mutants may play a role in the clinical severity of antithrombin deficiency. Mol Med 2012;18:762–70.

Int J Hematol (2014) 99:53–56
DOI 10.1007/s12185-013-1485-7

ORIGINAL ARTICLE

Distribution of serum erythropoietin levels in lower risk myelodysplastic syndrome cases with anemia

Kumi Nakazaki · Yasuhito Nannya · Mineo Kurokawa

Received: 19 September 2013 / Revised: 21 November 2013 / Accepted: 21 November 2013 / Published online: 5 December 2013

Abstract International guidelines for myelodysplastic syndrome (MDS) state that the standard therapy for lower risk MDS patients with symptomatic anemia of serum erythropoietin (EPO) <500 IU/L is erythroid-stimulating agents (ESAs). The objective of this study is to examine the distribution of EPO levels in lower risk MDS patients, and to inquire into the relationship of EPO distribution to hemoglobin levels and transfusions. Twenty cases of lower risk MDS (low or intermediate-1 by the International Prognostic Scoring System) with hemoglobin level <90 g/L at our institution were enrolled. Eight received more than two units of transfusions per month. Median hemoglobin level was 78 g/L. EPO levels ranged between 26.4 and 11300 IU/L (median 645 IU/L), including 10 cases (50 %) with >500 IU/L. EPO levels were inversely correlated to hemoglobin levels, especially in the cases without transfusion support ($p < 0.001$, $R = 0.92$). The rate of the cases with EPO <500 IU/L was significantly higher in the group without transfusion than the others ($p = 0.020$). Considering that, in Japan, the indication for transfusion is around 70 g/L of hemoglobin for chronic diseases, it may be possible to improve anemia in a subset of lower risk MDS cases by administration of ESAs before transfusions are required.

Keywords Myelodysplastic syndrome · Anemia · Serum erythropoietin

K. Nakazaki · Y. Nannya · M. Kurokawa (✉)
Department of Hematology and Oncology, Graduate School of Medicine, The University of Tokyo, 7-3-1 Hongo, Bunkyo-ku, Tokoyo 113-8655, Japan
e-mail: kurokawa-tky@umin.ac.jp

Introduction

International guidelines for myelodysplastic syndrome (MDS) show that the standard therapy for lower risk MDS patients with symptomatic anemia and serum erythropoietin (EPO) <500 IU/L is erythroid-stimulating agents (ESAs) [1–5]. However, only a few papers showed distribution of EPO levels of MDS patients in Japan before proposal of the International Prognostic Scoring System (IPSS) and the 2008 World Health Organization (WHO) classification prognostic scoring system (WPSS). They did neither distinguish lower risk MDS group, nor inquire into relationship to transfusions [6–8]. The objective of this study is to examine the distribution of EPO levels in lower risk MDS patients, and to investigate its relationship to hemoglobin levels and transfusions in our facility.

Materials and methods

Lower risk MDS cases (low or intermediate-1 by IPSS) with hemoglobin levels below 90 g/L at our institution were enrolled since June 2011 until June 2012, and serum EPO levels were measured by radioimmunoassay. This study was approved by the ethics board of The University of Tokyo and written informed consents were obtained in all the cases.

T test was applied to detect the difference of EPO levels among sex and transfusion dependency. The difference of the rate of the cases with EPO levels below 500 IU/L between the groups with or without transfusion was analyzed by Fisher's exact test. Pearson's correlation coefficient analysis was conducted for comparing age, hemoglobin levels, and IPSS-RA to EPO levels, respectively. Relation of WPSS to EPO levels was analyzed by polychoric correlation coefficient analysis.